

CHAPTER 1: INTRODUCTION[§]

1.1: METAL COMPLEXES AS DNA-BINDING AGENTS

DNA is the library of the cell, simultaneously storing and dispensing the information required for life. Molecules that can bind and react with specific DNA sites provide a means to access this cellular information. Over the past fifty years, small molecules that bind DNA have shown significant promise as diagnostic probes, reactive agents, and therapeutics. Naturally, a tremendous amount of attention has focused on the design of organic DNA-binding agents.¹ However, over the past twenty five years, some of this focus has shifted to another class of non-covalent DNA-binding agents: substitutionally inert, octahedral transition metal complexes.

At first glance, transition metal complexes seem an odd choice for DNA molecular recognition agents. Certainly, Nature herself offers very little precedent in this regard. With few exceptions, biological transition metals are confined to coordination sites in proteins or cofactors, not in discrete, free-standing coordination complexes.² Further, the cell generally employs organic moieties for the binding and recognition of DNA. Yet despite the lack of many natural examples, transition metal complexes offer two singular advantages as DNA-binding agents. First and foremost, coordination complexes offer a uniquely modular system. The metal center acts in essence as an anchor, holding in place a rigid, three-dimensional scaffold of ligands that can, if desired, bear recognition elements. The DNA-binding and recognition properties of a complex can thus be varied relatively easily via the facile interchange of ligands. Second, transition metal centers benefit from rich photophysical and electrochemical properties,

[§] Adapted from Zeglis, B. M.; Pierre, V. P.; Barton, J. K. Metallointercalators and metalloinsertors. *Chem. Comm.* **2007**, 4565–4579.

thus extending their utility far beyond that of mere passive molecular recognition agents. Indeed, these characteristics have allowed metal complexes to be used in a wide range of capacities, from fluorescent markers to DNA foot-printing agents to electrochemical probes.³

With very few exceptions, non-covalent, DNA-binding metal complexes share a set of fundamental characteristics. All are kinetically inert, a requisite trait due to the paramount importance of stability. Indeed, the vast majority of complexes are d^6 octahedral or d^8 square-planar. In addition, most exhibit a rigid or mostly rigid three-dimensional structure, an important facet considering that in many cases undue fluxionality could negate recognition. Moreover, the stereochemistry of a complex can dramatically influence recognition and specificity, an understandable notion given the chirality of the DNA target. Finally, most of the complexes that have been prepared are, by design, photochemically or photophysically active, properties that confer tremendous utility in probing metal complex-DNA interactions and nucleic acid structure.

1.2: A STRUCTURAL INTRODUCTION TO DNA

Before embarking on our discussion of the binding and recognition of DNA, a brief description of the structure of DNA may be helpful. DNA is a polymer of individual deoxyribonucleotides, each of which is composed of a heterocyclic base, a ribose sugar, and a phosphate (**Figure 1.1**). The most common form of DNA (and the form addressed almost exclusively in these pages) is the double-stranded, anti-parallel, right-handed double helix termed B-DNA, though the less common, right-handed A-form and left-handed Z-form will occasionally enter the discussion.^{4,5} Within the polynucleotide

assembly, the heterocyclic bases – adenine (A), guanine (G), cytosine (C), and thymine (T) – are bound to the sugars in an *anti* orientation with a disposition perpendicular to the helical axis. The base pairs collectively form a central π -stack that runs parallel to the helical axis between the two strands of the sugar-phosphate backbone. Each base forms hydrogen bonds with its complement on the opposite, anti-parallel strand, adenine with thymine and cytosine with guanine. The rise per base is 3.4 Å, and there are ten base pairs per helical turn. Surrounding the central base stack, the polyanionic sugar-phosphate backbone forms two distinct grooves, a wide major groove and a narrow minor groove. All of these structural characteristics can and have been exploited for molecular recognition.

1.3: EARLY WORK ON DNA-BINDING METAL COMPLEXES

The earliest research into the interactions between metals and DNA focused almost exclusively on the binding strength and location of metal-aquo ions, both those with and without biological significance.⁶ Perhaps as a result of these studies, the potential utility of metal-DNA interactions was realized early on. For example, melting temperature measurements for DNA in the presence of each of the first row transition metal ions were obtained to assess which metal ions stabilize or destabilize the duplex,⁷ and the use of uranyl-bound nucleosides was investigated as a possible tool for electron microscopy-based DNA sequence determination.⁸ Moreover, studies of the binding of mercury to non-thiolated and thiolated guanosine residues also further portended the

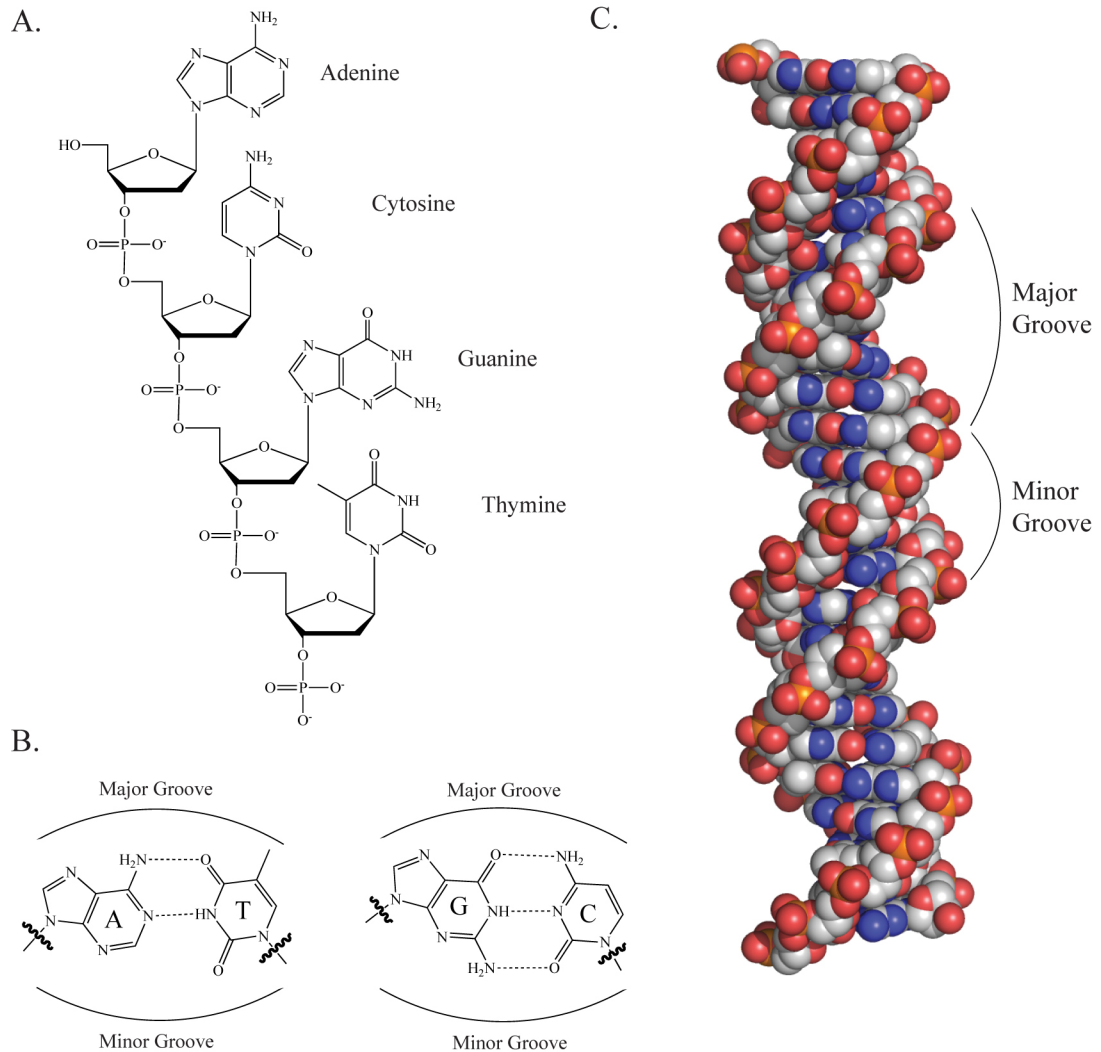


Figure 1.1: Deoxyribonucleic Acid. (A) Structures of the 4 natural DNA bases attached to the sugar phosphate backbone. (B) The Watson-Crick base pairs with major and minor grooves illustrated. (C) Model of double-stranded, B-form DNA. The major and minor grooves are indicated. Carbon, oxygen, nitrogen, and phosphorus atoms are grey, red, blue, and orange, respectively.

growing interest in metals as DNA probes.⁹ Importantly, these studies all focused upon the coordination of metal ions to DNA and as such employed either aquo-ions or complexes with open coordination sites. Our interest, however, is in the non-covalent binding of coordinatively saturated metal complexes to DNA. With respect to this area, clues suggesting the interaction of inert metal complexes and DNA were evident as early as the 1950s, most notably in F.P. Dwyer's work on the biological activity of metal polypyridyl complexes.¹⁰ Simple tris(chelate) complexes of Ru(II) and Ni(II) were found to have antiviral and bacteriostatic activities, in some cases with stereoselective biological activity (**Figure 1.2**).

It was not until the mid-1970s, however, that a progenitor non-covalent DNA-binding complex was prepared by S. J. Lippard and co-workers.¹¹ During their work on the binding of metals to thiolated bases, it was observed that the planar complex $\text{Pt}(2,2',2''\text{-terpyridine})(\text{Cl})^+$ induced a spectral shift for 4-thiouridine in the presence of tRNA. Follow up studies, this time using $\text{Pt}(\text{terpyridine})(\text{SCH}_2\text{CH}_2\text{OH})^+$ to eliminate the labile coordination site, employed a variety of techniques to establish the intercalative binding mode of the complex with DNA. X-ray fiber diffraction patterns provided further evidence for intercalation, revealing a periodicity of one platinum unit every 10 angstroms (every other base pair) and a partial un-winding of the phosphate backbone.¹² Subsequent investigations expanded the family of intercalators to include other complexes with planar heterocyclic ligands, $\text{Pt}(\text{bpy})(\text{en})^{2+}$ and $\text{Pt}(\text{phen})(\text{en})^{2+}$, established binding constants in the realm of $10^4\text{--}10^5 \text{ M}^{-1}$ for the family with DNA base pairs, and probed the effects of sequence context and ionic strength on intercalation.¹³

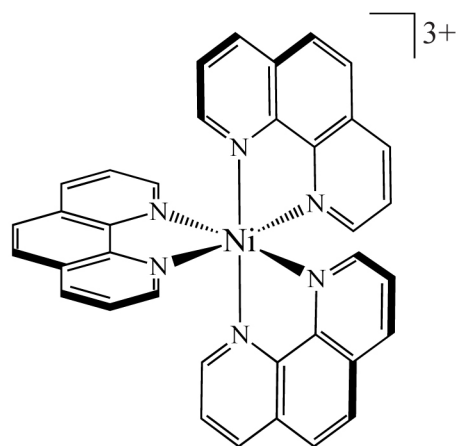
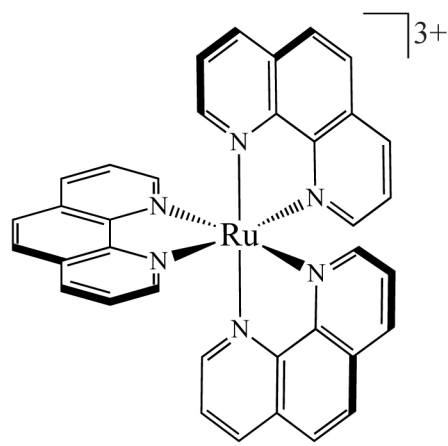
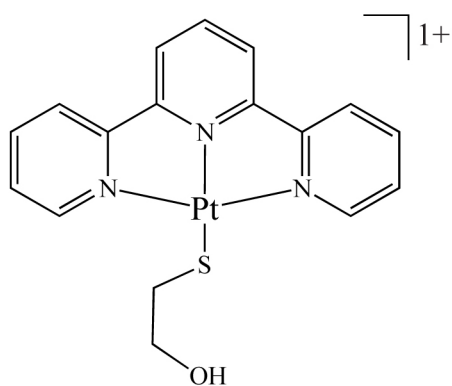
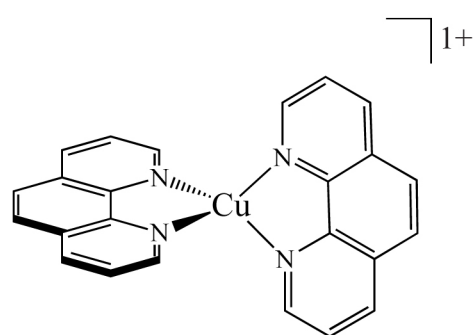

 $\Delta\text{-}[\text{Ni}(\text{phen})_3]^{2+}$

 $\Delta\text{-}[\text{Ru}(\text{phen})_3]^{2+}$

 $[\text{Pt}(\text{terpy})(\text{SCH}_2\text{CH}_2\text{OH})]^+$

 $[\text{Cu}(\text{phen})_2]^+$

Figure 1.2: Examples of early DNA-binding metal complexes. (Clockwise from top left): $\Delta\text{-}[\text{Ni}(\text{phen})_3]^{2+}$, $\Delta\text{-}[\text{Ru}(\text{phen})_3]^{2+}$, $[\text{Cu}(\text{phen})_2]^+$, $[\text{Pt}(\text{terpy})(\text{SCH}_2\text{CH}_2\text{OH})]^+$

Just as Lippard's platinum complexes laid the groundwork for future research on intercalative binding, the study of another complex, $\text{Cu}(\text{phen})_2^+$, in the lab of D. S. Sigman during the late 1970s and early 1980s unearthed the rich chemistry of groove-binding metal complexes.¹⁴ The complex was serendipitously discovered to degrade DNA during investigations into the inhibition of *E. coli* DNA polymerase by 1,10-phenanthroline, and it was soon learned that the DNA cleavage reaction was oxygen-dependent.¹⁵ Product isolation and analysis led to a proposed mechanism that suggested minor-groove binding by $\text{Cu}(\text{phen})_2^+$ formed *in situ*, a hypothesis later confirmed through elegant labeling experiments.^{16, 17} Additional reactivity studies revealed that the complex binds and cleaves not only B-form duplex DNA but also A-form DNA, RNA, and other folded nucleic acid structures.¹⁸

1.4: NATURE'S EXAMPLE: FE-BLEOMYCIN

It is important to address, at least briefly, Nature's lone example of a non-covalent DNA-binding metal complex: metalbleomycin. First isolated from *Streptomyces verticillus* in the late 1960s, bleomycins are a widely-studied family of glycopeptide antibiotics that have been used successfully in the treatment of some forms of cancer.¹⁹ The structure of bleomycins can be broken down into three domains: a metal-binding domain containing a pyrimidine moiety and five nitrogen atoms for octahedral metal coordination, a peptide linker region bearing a disaccharide side-chain, and a bithiazole unit with an appended, positively charged tail (**Figure 1.3**). While the metal-binding

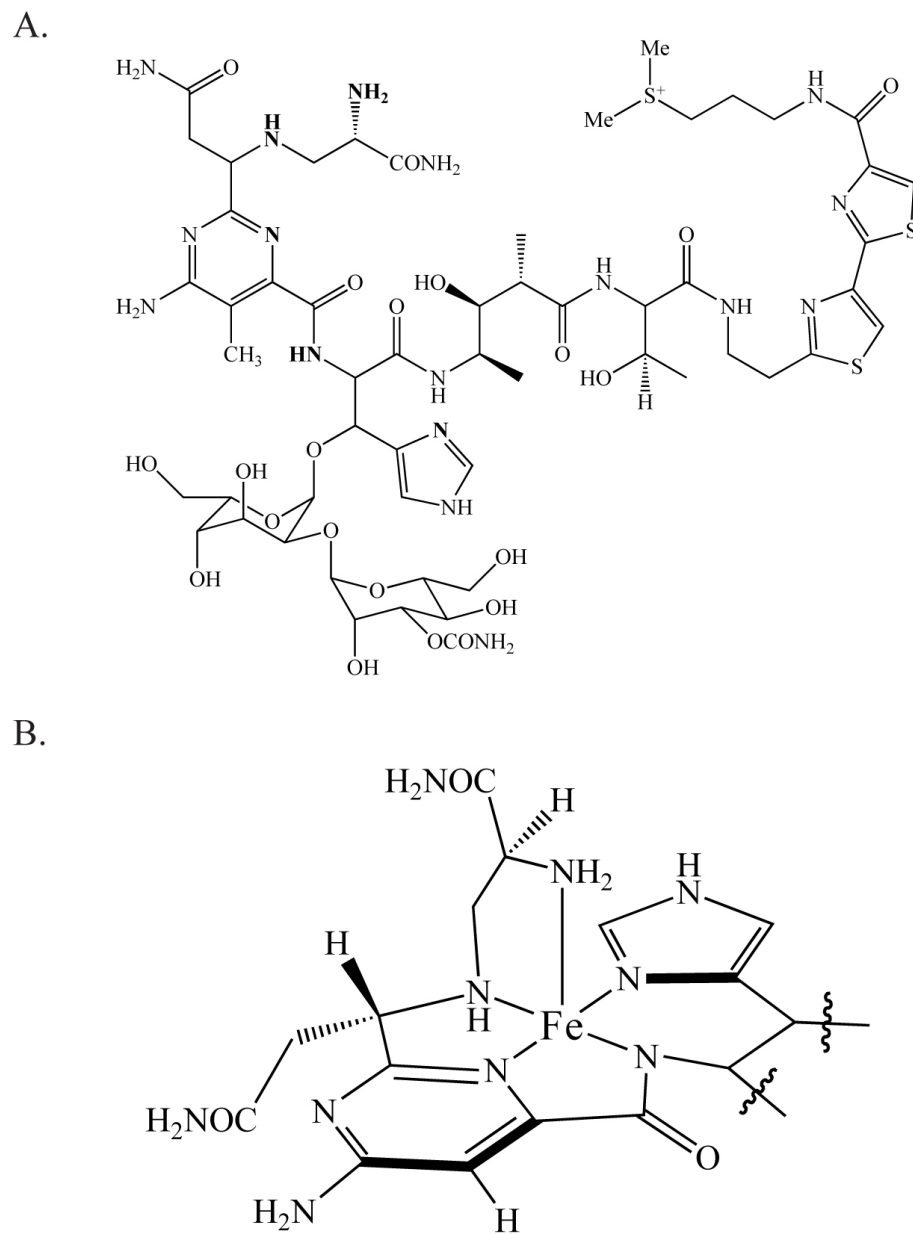


Figure 1.3: Bleomycin. Structures of (A) apo-bleomycin A₂ with coordinating nitrogens in bold and (B) the Fe coordination environment of bleomycin

region can coordinate a variety of metals, including Zn(II), Cu(II), and Co(III), the majority of research has focused on Fe-bleomycin complexes.²⁰ Significantly, exposure of the Fe bleomycin complex to oxygen and a reductant leads to the formation of activated bleomycin, a species that can, in turn, affect both single-stranded and double-stranded DNA cleavage via 4'-hydrogen atom abstraction by a high valent Fe-oxo species.

Metallobleomycins bind DNA via the minor groove, though neither affinity nor specificity is particularly high. Over the past twenty years, extensive synthetic and spectroscopic studies have helped elucidate the contribution of each structural moiety to DNA-binding and reactivity.²⁰ The bithiazole subunit and positively-charged tail are considered to play the most important roles in DNA-binding. The charge of the cationic tail is generally agreed to provide electrostatic impetus for binding. The role of the bithiazole, however, is subject to considerably more debate. And while the bulk of the evidence suggests that this moiety intercalates between base-pairs neighboring the binding site of the complex^{21, 22}, others have suggested that the bithiazole interacts with the DNA primarily in the minor groove.²³ To continue, hydrogen-bonding of the pyrimidine moiety in the metal-binding region is thought to help confer 5'-G-Py-3' cleavage selectivity.²⁴ The definitive roles of the linker region and disaccharide have proven more subtle and elusive, with the linker region likely of conformational importance and the disaccharide having been assigned roles ranging from DNA binding to metal chelation to cellular uptake and localization.

Finally, it is also both interesting and important to note that metallobleomycins, unlike many of the metal complexes discussed below, are exquisitely sensitive to

structural changes, for attempts to alter any of the domains have been met with dramatically reduced binding and cleavage efficiencies.²⁰

1.5: TRIS(PHENANTHROLINE) COMPLEXES

The earliest work on the DNA-binding of octahedral metal centers focused on tris(phenanthroline) complexes of ruthenium, cobalt, zinc, and nickel.²⁵⁻³⁰ Extensive photophysical and NMR experiments suggested that these complexes bound to DNA via two distinct modes: (a) hydrophobic interactions in the minor groove and (b) partial intercalation of a phenanthroline ligand from the major groove. Perhaps more important than the discovery of these dual binding modes, however, was the revelation these complexes provided regarding the importance of chirality in the binding of octahedral metal complexes to DNA.³¹ In the case of $\text{Ru}(\text{phen})_3^{2+}$, for example, the Δ -enantiomer is preferred in the intercalative binding mode, while the complementary Λ -enantiomer is favored in the minor groove binding mode (**Figure 1.4**). In subsequent years, it was discovered that metal centers bearing more sterically demanding phenanthroline ligand derivatives, such as diphenylphenanthroline (DIP), display even more dramatic chiral discrimination. Luminescence and hypochromism assays have revealed enantioselective binding on the part of $\text{Ru}(\text{DIP})_3^{2+}$: the Δ -enantiomer binds enantiospecifically to right-handed B-DNA, while the Λ -enantiomer binds only to left-handed Z-DNA.³² This enantiospecificity has been exploited to map left-handed Z-DNA sites in supercoiled plasmids using Λ - $\text{Co}(\text{phen})_3^{3+}$.³³ Indeed, the trend in enantiomeric selectivity for octahedral tris(chelate) complexes — matching the symmetry of the

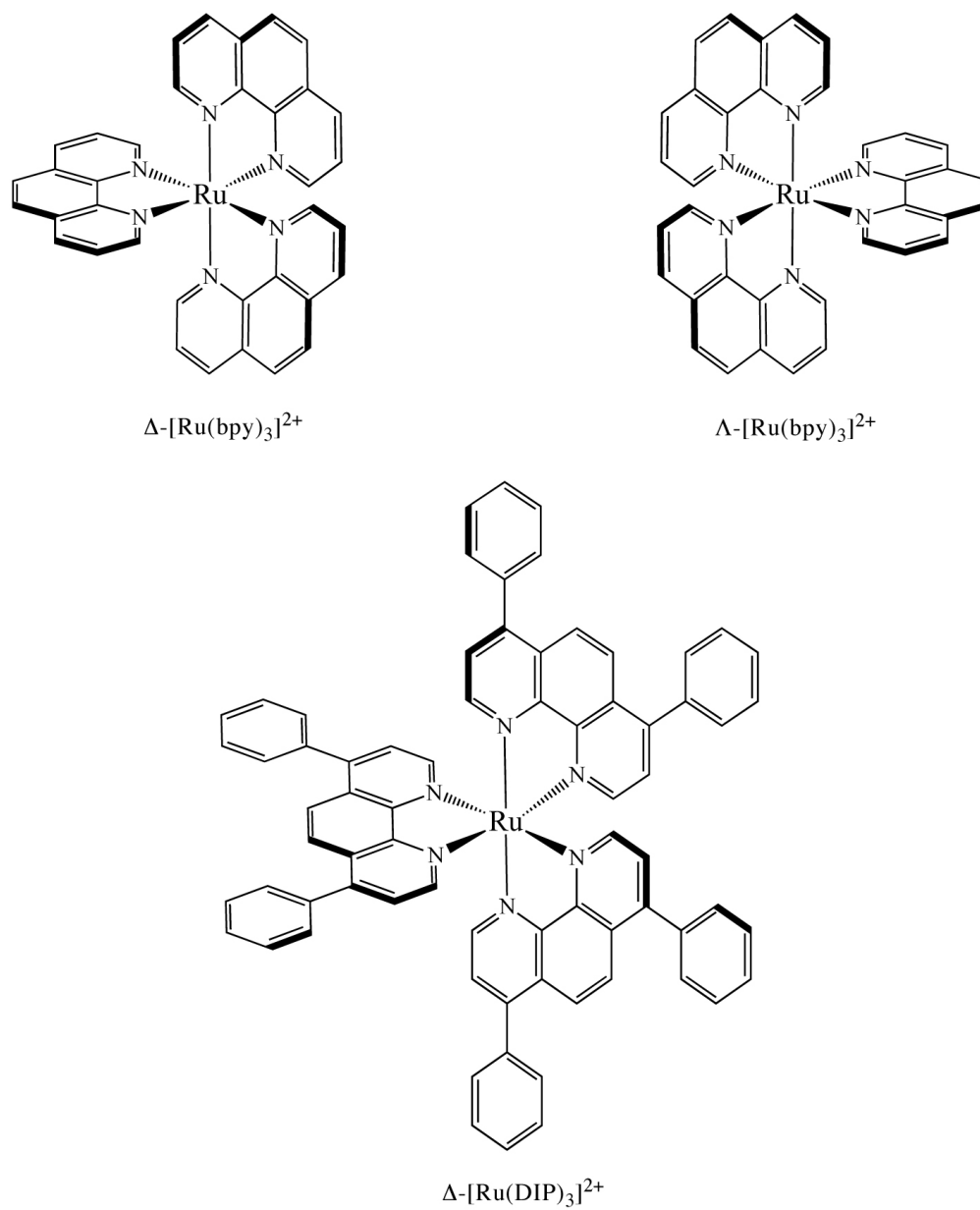


Figure 1.4: Ruthenium tris(phenanthroline) complexes

complex to that of DNA helix — has repeatedly and consistently been observed for non-covalent DNA-binding complexes developed in the years since these initial discoveries.³⁴

These earliest tris(phenanthroline) complexes do not, of course, represent the only examples of complexes that bind DNA via the minor or major grooves. The extensively studied $\text{Cu}(\text{phen})_2^+$, for instance, has been shown to bind DNA via the minor groove. Indeed, these particular groove-binding complexes not only bind DNA but also cleave the macromolecule in the presence of hydrogen peroxide.^{16, 35} Metal complexes that bind in the groove have come a long way since these first studies and are now quite sophisticated. Turro, for instance, developed an artificial photonuclease by linking the metallogroove-binder $\text{Ru}(\text{bpy})_3^{2+}$ to an electron-acceptor chain containing two viologen units. Interestingly, the chemistry of metallogroove-binders also extends to supramolecular self-assembly. Following the initial work of Lehn on the interaction and cleavage of DNA with a cuprous double-helicate,³⁶ Hannon and coworkers designed a triple-helicate capable of recognizing three-way junctions in DNA. This intricate recognition has recently been characterized by single crystal X-ray crystallography.³⁷⁻³⁹

1.6: METALLOINTERCALATORS

1.6.1: GENERAL ARCHITECTURE OF THE BINDING MODE

Intercalators are small organic molecules that unwind DNA in order to π -stack between two base pairs. Metallointercalators, it then follows, are metal complexes that bear at least one intercalating ligand. As their name suggests, these ligands, oriented parallel to the base pairs and protruding away from the metal center, can readily π -stack in the DNA duplex. Further, upon binding, the ligands behave as a stable anchor for the

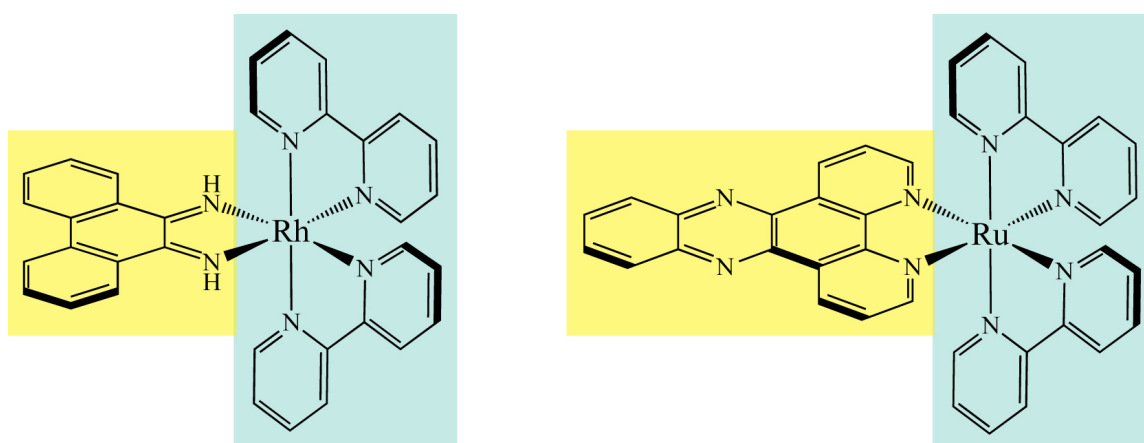
 $\Delta\text{-Rh}(\text{bpy})_2(\text{phi})^{3+}$ $\Delta\text{-Ru}(\text{bpy})_2(\text{dppz})^{2+}$

Figure 1.5: Chemical structure of $\Delta\text{-Rh}(\text{bpy})_2(\text{phi})^{3+}$ and $\Delta\text{-Ru}(\text{bpy})_2(\text{dppz})^{2+}$. The intercalating ligands are highlighted in yellow, the ancillary ligands in cyan.

metal complex with respect to the double helix and direct the orientation of the ancillary ligands with respect to the DNA duplex. Two well-known examples of intercalating ligands are phi (9,10-phenanthrenequinone diimine) and dppz (dipyrido[3,2-*a*:2',3'-c]phenazine) (**Figure 1.5**).³

Ligand intercalation was first demonstrated by photophysical studies.⁴⁰⁻⁴⁶ However, it was not until extensive NMR studies⁴⁷⁻⁵⁰ and high resolution crystal structures had been performed that the structural details of this binding mode were properly illuminated.⁵¹ Metallointercalators bind DNA from the major groove, with the intercalating ligand acting in effect as a new base pair. Intercalation results in a doubling of the rise and a widening of the major groove at the binding site. However, beyond these changes, this interaction distorts only minimally the structure of DNA. In the case of B-DNA, for example, the sugars and bases all maintain their original C_{2'}'-endo and *anti* conformations, respectively. Indeed, only the opening of the phosphate angles, not any base or sugar perturbations, is necessary for intercalation.

Three crystal structures of a metal complex intercalated within a duplex, two containing an octahedral rhodium complex bound to an oligonucleotide and one a square-planar platinum complex bound to a paired dinucleotide, each demonstrate that intercalation occurs via the major groove.⁵¹⁻⁵³ Yet this may not always be the case. NMR studies indicate that metal complexes bearing dpq (dipyrido[2,2-*d*:2',3'-*f*]quinoxaline), a close analogue of dppz lacking the terminal aromatic ring, favor binding via the minor groove.⁵⁴⁻⁵⁶ Whether this binding by the more hydrophobic complex involves one or two binding modes, perhaps groove-binding from the minor groove along with intercalation, still needs to be confirmed.

1.6.2: EXPLOITING THE PHOTOPHYSICAL AND PHOTOCHEMICAL PROPERTIES OF METALLOINTERCALATORS

By design, metallointercalators are coordinatively saturated and substitutionally inert such that no direct coordination with DNA bases occurs. Nonetheless, they often possess rich photochemistry and photophysics that have been advantageously exploited both to probe their interaction with DNA and interrogate further various aspects of nucleic acid chemistry. The most studied example is almost certainly the molecular light switch complex, $\text{Ru}(\text{phen})_2(\text{dppz})^{2+}$. This ruthenium complex shows solvatochromic luminescence in organic solutions. In aqueous solutions, however, it does not luminesce, because water deactivates the excited state through hydrogen-bonding with the endocyclic nitrogen atoms of the intercalating ligand. Remarkably, however, the complex luminesces brightly upon the addition of duplex DNA (**Figure 1.6**). In this case, the metal complex intercalates into the DNA, and the surrounding duplex prevents water from gaining access to the intercalated ligand; thus, the DNA has created a local region of aprotic ‘solvent’ in which the metal complex, now free of any hydrogen bonds, can display its characteristic luminescence.^{40, 57, 58}

Although there has been some debate over the binding orientation of $\text{Ru}(\text{phen})_2(\text{dppz})^{2+}$, it has now been established that the complex intercalates via the major groove. Direct competition titrations against both a minor groove binder (distamycin) and a well-characterized major groove intercalator ($\Delta\text{-}\alpha\text{-Rh}[(\text{R,R})\text{-Me}_2\text{trien}](\text{phi})^{3+}$, *vide infra*) clearly demonstrate that the molecular light switch intercalates via the major groove with a slight preference for poly-d(AT) regions over poly-d(GC) tracts.⁵⁹ This conclusion is further supported by detailed NMR studies

performed with complexes bearing selectively deuterated dppz ligands. The latter investigations, together with the observed biexponential decay of the luminescence of $\text{Ru}(\text{phen})_2(\text{dppz})^{2+}$, further stipulate the presence of two populations with slightly different intercalation geometries. Many analogues of the popular molecular light switch, such as Nordén's threading bis-intercalators,^{60, 61} have been synthesized, and their photophysics extensively studied and reviewed.⁶²

While ruthenium and dppz-based metallointercalators have proven to be powerful molecular light switches for the detection of DNA, rhodium intercalators have been shown to be efficient agents for photoactivated DNA strand cleavage. Importantly, this reactivity enables us to mark directly the site of intercalation and to characterize the recognition properties of each metallointercalator. In this case, the most well studied examples are rhodium complexes employing the phi ligand as the intercalating ligand, such as $\text{Rh}(\text{bpy})_2(\text{phi})^{3+}$, $\text{Rh}(\text{phen})_2(\text{phi})^{3+}$, and $\text{Rh}(\text{phi})_2(\text{bpy})^{3+}$.⁶³

In many cases, DNA cleavage is observed after irradiation of the DNA-bound metal complex at short wavelengths (313–325 nm). This irradiation prompts the formation of an intercalating ligand-based radical that abstracts a hydrogen atom from the adjacent deoxyribose ring.⁴³ Subsequent degradation of the resultant sugar radical then leads to direct DNA strand scission. In the absence of dioxygen, the photolysis of intercalated rhodium complexes leads to the formation of 3'- and 5'-phosphate terminated strands as well as a free base. To contrast, in the presence of dioxygen, direct strand cleavage still occurs but instead produces a 5'-phosphate terminated strand, a 3'-phosphoglycaldehyde terminated strand, and a base propenoic acid. These observations

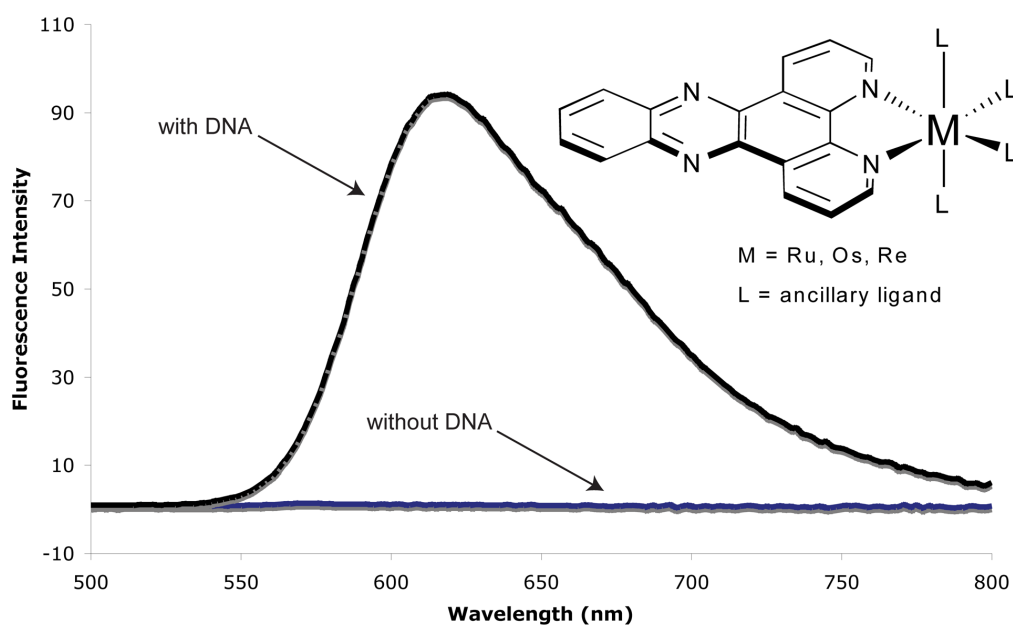


Figure 1.6: The light-switch effect of dppz-based metallointercalators. A representative plot of the effect of DNA on the luminescence of complexes of the general form $M(dppz)(L)_4$. In the absence of DNA (blue), hydrogen-bonding to the endocyclic phenazine nitrogens deactivates the fluorescence of the molecule. In the presence of DNA (black), the phenazine nitrogens are protected from water, and the complexes exhibit intense fluorescence.

are consistent with previously observed chemistry at the C3' position of the sugar. However, since both an atomic resolution crystal structure and a solution NMR study of a metal complex intercalated in the major groove of DNA indicate that the C2' hydrogen of the neighboring sugars is closer to the intercalating ligand than the C3' hydrogen, we propose that initially, the photoactivated intercalator abstracts the C2' hydrogen of the sugar. This is immediately followed by hydrogen migration to form the C3' radical and subsequent degradation of the sugar ring.

Although rhodium complexes efficiently cleave DNA upon photoactivation, many research laboratories find more convenient the use of DNA cleavage agents that cut without irradiation.⁶⁴ This can be achieved through the use of a bifunctional metallointercalator – peptide chimera in which a metal-coordinating peptide is covalently attached to $\text{Rh}(\text{phen})_2(\text{bpy}')^{3+}$ (**Figure 1.7**). The metallointercalator acts as a targeting vector that delivers the metallopeptide to the sugar-phosphate backbone. The latter then promotes hydrolytic DNA strand cleavage.

In a similar approach, luminescent DNA cross-linking probes were achieved using bifunctional ruthenium intercalators conjugated to short peptides.⁶⁵ In the presence of an oxidative quencher, irradiation of the intercalated $\text{Ru}(\text{phen})(\text{bpy}')(\text{dppz})^{2+}$ oxidizes the oligonucleotide. The nearby tethered peptide then crosslinks with the oxidized site of the DNA. Although delivery of the peptide by the metallointercalator is not essential for cross-linking, this technique advantageously yields cross-linking adducts that are luminescent and are thus easily detectable. Furthermore, these cross-links may resemble those found *in vivo* under conditions of oxidative stress.

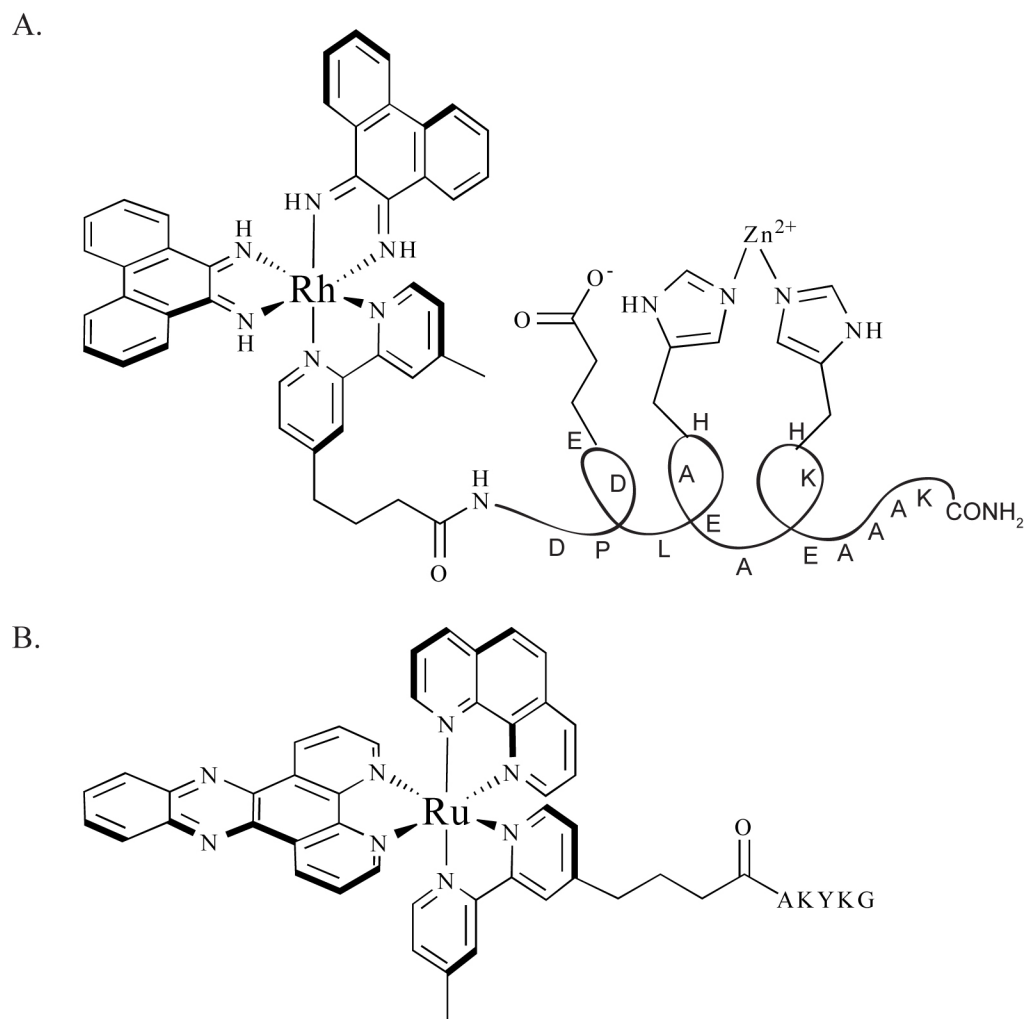


Figure 1.7: Metallointercalator conjugates. Chemical structures of (A) an artificial nuclease and (B) a luminescent cross-linking agent

1.6.3: SHAPE-SELECTIVE RECOGNITION

On the whole, metallointercalators are structurally rigid molecules with well-defined symmetry, making them particularly well suited for selective molecular recognition of specific DNA sequences. Importantly, because of the general rigidity of the complexes, both the overall shape and ancillary ligands of these complexes can also be exploited in the development of useful agents.

Perhaps not surprisingly, stereochemistry is of utmost importance in the construction of site-specific recognition agents. Indeed, one of the earliest findings in this field was the necessity of matching the chirality of the metallointercalator with that of the double helix: the Δ -enantiomer of the metal complex preferentially binds to right-handed B-DNA. This enantioselective discrimination is primarily steric in nature and depends on the size of the ancillary ligands relative to that of the DNA groove. For instance, poor enantioselectivity is observed with metallointercalators bearing small ancillary ligands such as phenanthroline and bipyridine, whereas complete enantiospecificity is achieved with bulkier ancillary ligands such as DPB (4,4'-diphenyl-bipyridine).^{66, 67} The Δ -enantiomer of $\text{Rh}(\text{phi})(\text{DPB})_2^{3+}$, for example, readily cleaves the sequence 5'-CTCTAGAG-3' upon photoactivation, but no intercalation or cleavage is observed with the Λ -enantiomer, even with a thousand-fold excess of metallointercalator (**Figure 1.8**). For Z-DNA, which is a left-handed helix, little enantioselectivity for chiral metal complexes is observed because of the very shallow, almost convex major groove;²⁵ hence the Λ -isomer, which cannot bind at all to B-form DNA, becomes a selective probe for Z-DNA.

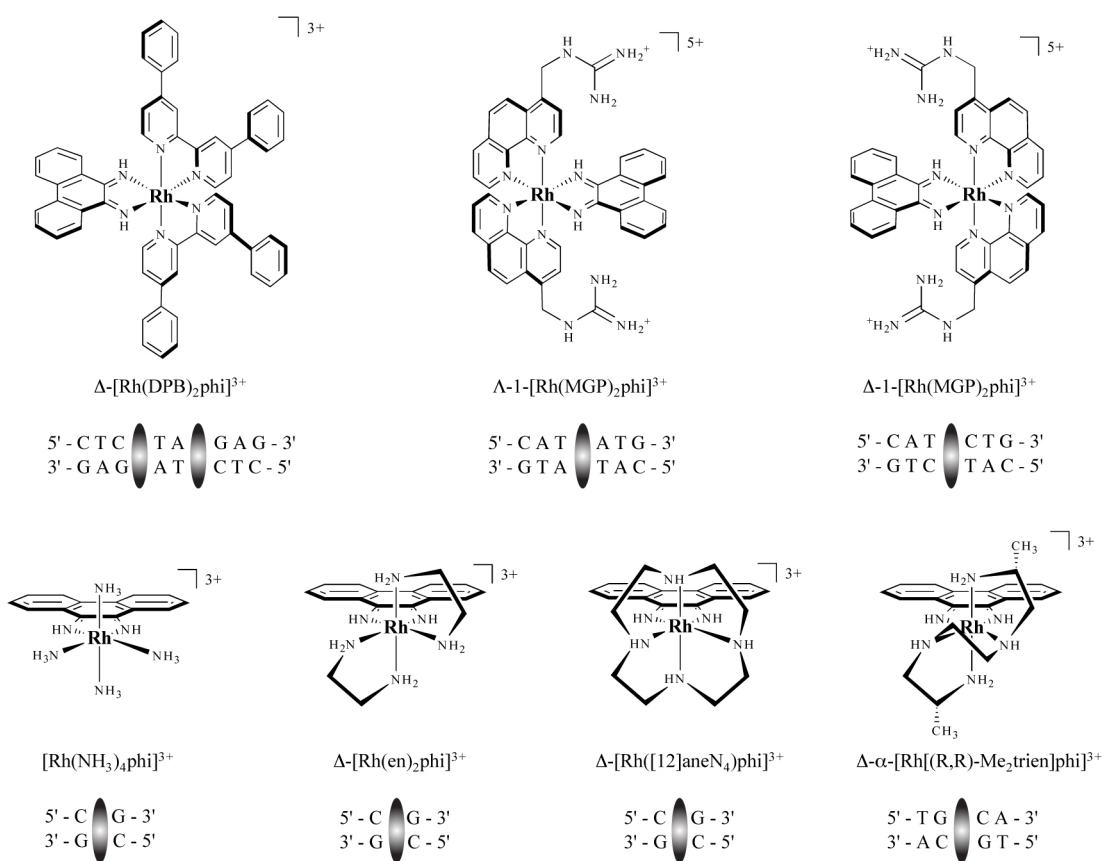


Figure 1.8: Sequence-specific metallointercalators and their target sequences. The name and recognition site of each metallointercalator is shown below the chemical structure of complex. The shaded grey ovals indicate the precise location of intercalation.

As a monomer, $\Delta\text{-Rh}(\text{phi})(\text{DPB})_2^{3+}$ is geometrically capable of spanning only six base pairs; however, the metallointercalator is able to recognize a palindromic sequence eight base pairs long by dimerizing. The target sequence 5'-CTCTAGAG-3' can be considered as two overlapping 5'-CTCTAG-3' intercalation sites. Concomitant intercalation of two metal complexes, each at a central 5'-CT-3' of the 6-mer, favors stacking of the ancillary phenyls from both complexes over the central 5'-TA-3' step. This binding cooperativity, more common with DNA binding proteins, enhances the binding affinity of the second intercalator by 2 kcal. As a result, irradiation of the metallointercalators / DNA adduct cleaves both DNA strands with three base pairs separating the two cleavage sites.

The remarkable specificity and intricate binding mode of $\Delta\text{-Rh}(\text{phi})(\text{DPB})_2^{3+}$ enables it to inhibit efficiently the activity of *XbaI* restriction endonuclease at the palindromic site.⁴⁶ Notably, no comparable inhibition of *XbaI* has been achieved with any other metallointercalators, and $\Delta\text{-Rh}(\text{phi})(\text{DPB})_2^{3+}$ cannot inhibit restriction enzymes that bind different sites. Thus, metallointercalators have found use not only as probes for nucleic acid structures but also as mimics and, perhaps, inhibitors of DNA-binding proteins.

Interestingly, more moderate shape-based site recognition can be achieved with sterically smaller ancillary ligands like phenanthroline. $\text{Rh}(\text{phen})_2(\text{phi})^{3+}$, for instance, preferentially intercalates at sites with high propeller twisting toward the major groove.^{63, 68-70} This intercalator preferentially photocleaves 5'-Py-Py-Pu-3' sites and occasionally 5'-Pu-Py-Pu-3' sites but not 5'-Pu-Pu-Py-3' sites. Comparison of photocleavage experiment results with the crystal structures of several B-form oligonucleotides reveals a

direct correlation between the binding preference of $\text{Rh}(\text{phen})_2(\text{phi})^{3+}$ and the increased propeller twisting at the sites of intercalation. Opening of the major groove in the 5'-Py-Pu-3' sequence produces more steric leeway for the hydrogens of the ancillary phenanthroline ligands, thus enabling deeper intercalation by the metal complex. In the case of a 5'-Pu-Pu-Py-3' site, however, reduced propeller twisting creates a more sterically confining major groove at the intercalation site; in this instance, then, increased steric hindrance between the groove and the phenanthroline ligands pushes the intercalating phi ligand farther away from the DNA helical axis, thereby reducing the binding affinity of the complex.

Due to its unique properties, $\text{Rh}(\text{phen})_2(\text{phi})^{3+}$ has also been employed as a probe for RNA tertiary structure.^{42, 71-73} As discussed above, the complex can only intercalate from the major groove side of DNA, a property which prevents it from binding via the sterically-altered groove of duplex RNA and binding instead preferentially to triplex RNA. In this capacity, the rhodium complex is able to compete for binding at the TAT protein binding site in the immunodeficiency virus TAR RNA.⁷⁴ $\text{Rh}(\text{phen})_2(\text{phi})^{3+}$ efficiently binds and photocleaves the U24 base involved in the base-triplex of the RNA hairpin that is essential to TAT binding. The metal complex similarly competes with and inhibits the binding of the bovine BIV-TAT peptide to its RNA target site. Mutants of the RNA oligomer lacking the base triplex and which can therefore no longer bind the TAT peptide are likewise no longer targeted by the metallointercalator.

1.6.4: SEQUENCE RECOGNITION BASED ON FUNCTIONALITY

Selective recognition of a DNA sequence by a metallointercalator can also be achieved by matching the functionality of the ancillary ligands positioned in the major groove with those of the targeted base pairs. Specific targeting of the sequence 5'-CG-3', for instance, is achieved with the complexes $\text{Rh}(\text{NH}_3)_4(\text{phi})^{3+}$, $\text{Rh}([12]\text{aneN}_4)(\text{phi})^{3+}$ and $\Delta\text{-Rh}(\text{en})_2(\text{phi})^{3+}$.⁷⁵⁻⁷⁸ In these examples, recognition is ensured both by the C2 symmetry of the metal complexes and hydrogen bonding between the axial amines of the metallointercalators and the O6 atoms of the guanines. The Λ -enantiomer of $\text{Rh}(\text{en})_2(\text{phi})^{3+}$, in contrast, recognizes the sequence 5'-TA-3' due to van der Waals contact between the methylene groups on the backbone of the complex and the thymine methyls of the DNA.

The predictive design of sequence specific metallointercalators was expanded with $\Delta\text{-}\alpha\text{-Rh}[(\text{R,R})\text{-Me}_2\text{trien}](\text{phi})^{3+}$, a complex that specifically recognizes and photocleaves the sequence 5'-TGCA-3' (**Figure 1.9**).⁷⁹ The rhodium complex was designed to recognize this sequence via hydrogen bonding contacts between the axial ammine ligands and the O6 atoms of the guanines, as well as potential van der Waals contacts between the pendant methyl groups on the metal complex and the methyl groups on the flanking thymines. A high resolution NMR solution structure followed by the first crystal structure of a metallointercalator-DNA adduct later revealed at atomic resolution the details of the intercalation and recognition. In fact, it is because of the high sequence-specificity of this intercalator that a high resolution view of intercalation within a long DNA duplex could be obtained. In the DNA octamer containing the central 5'-TGCA-3'

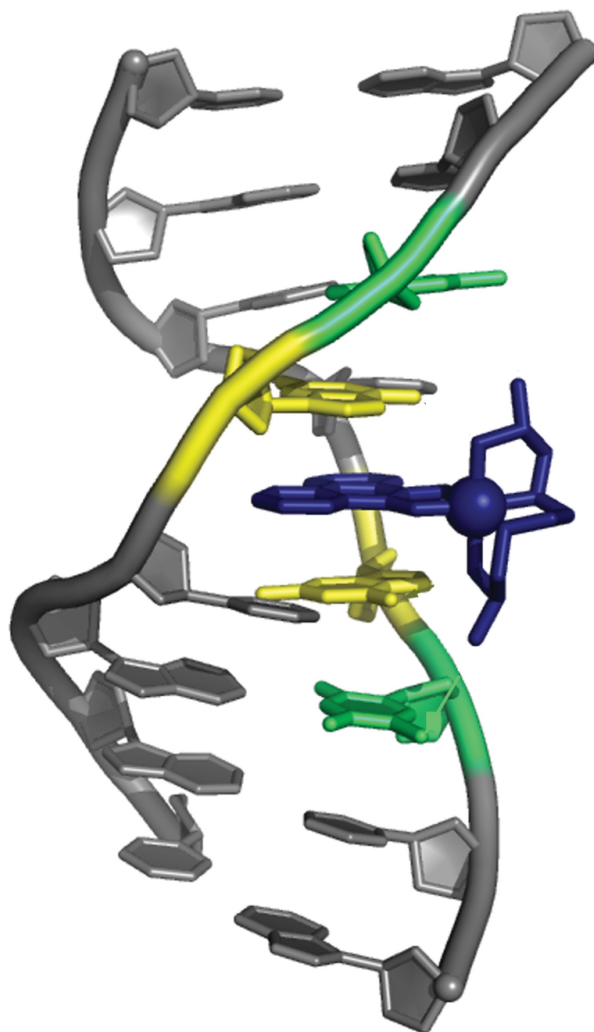


Figure 1.9: Crystal structure of the metallointercalator $\Delta\text{-}\alpha\text{-}[\text{Rh}[(\text{R,R})\text{-Me}_2\text{trien}]\text{phi}]^{3+}$ bound to its target sequence, 5'-TGCA-3'. The recognition is conferred by two sets of interactions: (1) hydrogen bonding between the axial amines of the complex and the O6 atoms of the guanines and (2) methyl-methyl interactions between the ligand methyl groups and those of the thymines.

site, the DNA unwinds to enable complete and deep intercalation of the phi ligand of the metal complex within the major groove. This results in a doubling of the rise at the intercalation site without any base ejection. The metallointercalator thus behaves as a newly added base pair that causes only minimal structural perturbation to the DNA. Furthermore, both the NMR study and crystal structure confirm that the sequence-specific recognition is, indeed, based on the anticipated hydrogen bonding and van der Waals interactions.

1.6.5: SEQUENCE RECOGNITION BASED ON SHAPE AND FUNCTIONALITY

Yet another metallointercalator provides an interesting example of sequence-specific recognition predicated on both shape *and* functionality. $1\text{-Rh}(\text{MGP})_2(\text{phi})^{5+}$, a derivative of $\text{Rh}(\text{phen})_2(\text{phi})^{3+}$ containing pendant guanidinium groups on the ancillary phenanthroline ligands, was designed to bind a subset of the sequences recognized by the latter complex, specifically those 5'-Py-Py-Pu-3' triplets flanked by two G•C base pairs. Hydrogen bonding between the guanidinium groups on the ancillary ligands and the O6 atoms of the flanking guanines was expected to confer this selectivity.^{80, 81} As predicted, NMR studies demonstrate that the Δ -enantiomer recognizes the sequence 5'-CATCTG-3' specifically.

Surprisingly, in spite of the large size of the ancillary ligands, the Δ -enantiomer also binds DNA and recognizes a different sequence, 5'-CATATG-3'. The expansive MGP ligands certainly prevent the left-handed isomer from entering the major groove of right-handed DNA. However, plasmid unwinding assays and NMR studies establish that the Δ -enantiomer of the metallointercalator binds DNA by unwinding it up to 70°. It is in

this conformation that the complex can span the entire six-base pair binding site and contact the N7 position of the flanking guanines with the pendant guanidinium groups. Replacing these flanking guanines with deazaguanines demonstrates that the absence of the N7 nitrogen atoms eliminates any site selectivity. Therefore, we can conclude that the guanidinium functionalities of the ancillary ligands are responsible for the recognition of the flanking guanines, whereas the shape of the metallointercalator enables the recognition of the “twistable” central 5'-ATAT-3' sequence.

Due to its high site-specificity, the Λ -enantiomer of this complex has found biological application as an inhibitor of transcription factor binding.⁸² In a manner similar to $\text{Rh}(\text{phen})_2(\text{phi})^{3+}$, Λ -1- $\text{Rh}(\text{MGP})_2(\text{phi})^{5+}$ can site-specifically inhibit the binding of a transcription factor to its activator recognition region. In competition experiments with yeast Activator Protein 1 (yAP-1), the metal complex was able to compete with the protein for a domain that included both the binding region of yAP-1 and that of Λ -1- $\text{Rh}(\text{MGP})_2(\text{phi})^{5+}$ at concentrations as low as 120 nM. This result represents one of the first hints at the therapeutic potential of rhodium intercalators, a notion strongly supported by subsequent investigations illustrating that $\text{Rh}(\text{phi})_2(\text{phen})^{3+}$ and other rhodium bis(quinone diimine) complexes inhibit transcription *in vitro*.^{83, 84}

1.7: METALLOINSERTORS

Without a doubt, the vast majority of non-covalent, DNA-binding metal complexes are either groove-binders or intercalators. However, the dearth of complexes that bind DNA via other means does not necessarily exclude the existence of alternative

modes. Indeed, L.S. Lerman, in his seminal article proposing intercalation as the DNA-binding mode for organic dyes, presciently proposed a third non-covalent binding mode: insertion.⁸⁵ A molecule, he posited, may bind “a DNA helix with separation and displacement of a base-pair.” While Lerman was addressing organic moieties, we can apply this thinking to metal complexes quite easily. Metalloinsertors, like metallointercalators, contain a planar aromatic ligand that extends into the base-stack upon DNA-binding. However, while metallointercalators unwind the DNA and stack their planar ligand between two intact base pairs, metalloinsertors separate and eject the bases of a single base pair, with their planar ligand acting as a π -stacking replacement in the DNA base stack.

Until very recently, no examples of DNA-binding insertors, neither metallic nor organic, had been reported. However, our research into mismatch-specific DNA-binding agents has led to the discovery of a family of rhodium complexes that bind DNA via this unique mode. These novel complexes have been dubbed metalloinsertors (**Figure 1.10**).

1.7.1: MISMATCHED DNA

1.7.1.1: STRUCTURE

Genomic fidelity is vital to cellular survival and replication. However, a wide variety of DNA defects can arise in the lifetime of a cell to threaten the fidelity of the genome.⁸⁶ Non-canonical base pairs, commonly known as single base mismatches, are one particularly deleterious class of DNA defects. Eight possible mismatches exist, each thermodynamically destabilized relative to the A•T and C•G Watson-Crick base pairs: A•A, A•C, A•G, C•C, C•T, G•G, G•T, and T•T (**Figure 1.11**).

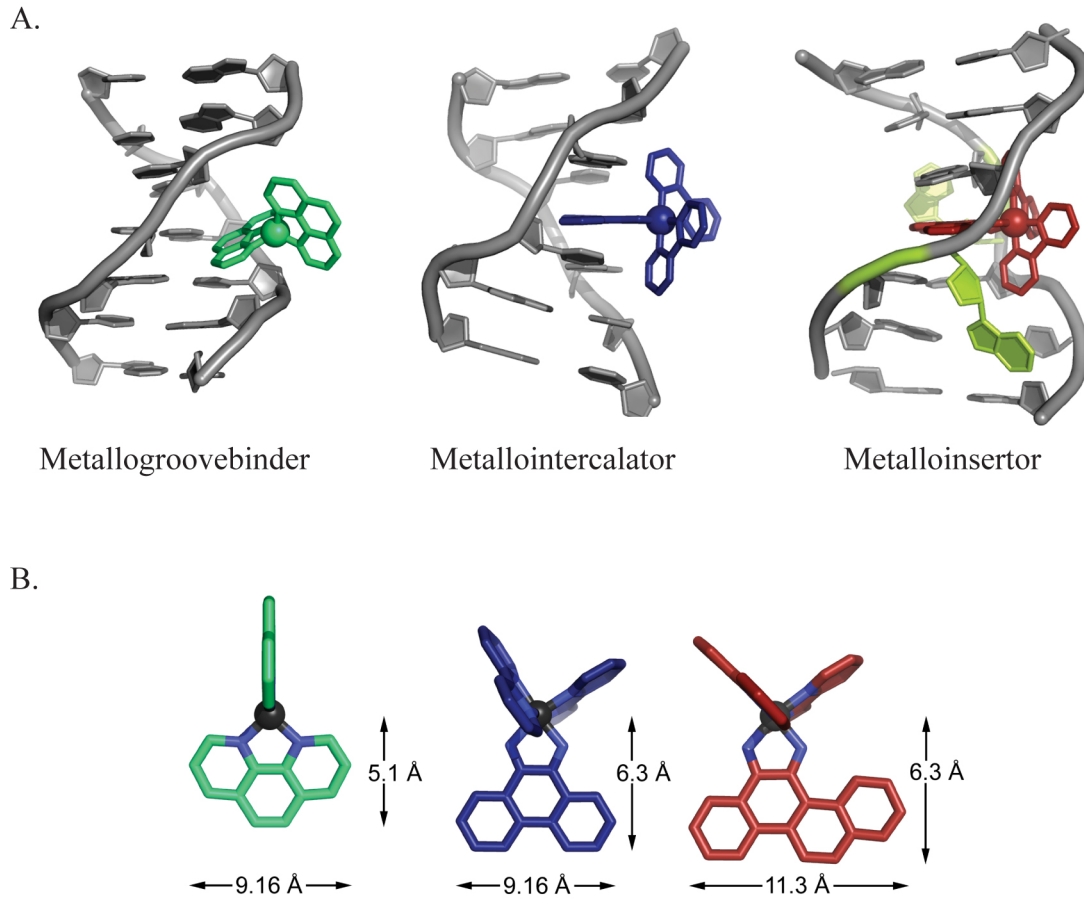


Figure 1.10: Three non-covalent binding modes for metal complexes and DNA. (A) Models of a metallo-groove-binder (green), metallointercalator (blue), and metalloinsertor (red) bound to DNA; (B) Representative dimensions of a metallo-groove-binder (green), metallointercalator (blue), and metalloinsertor (red)

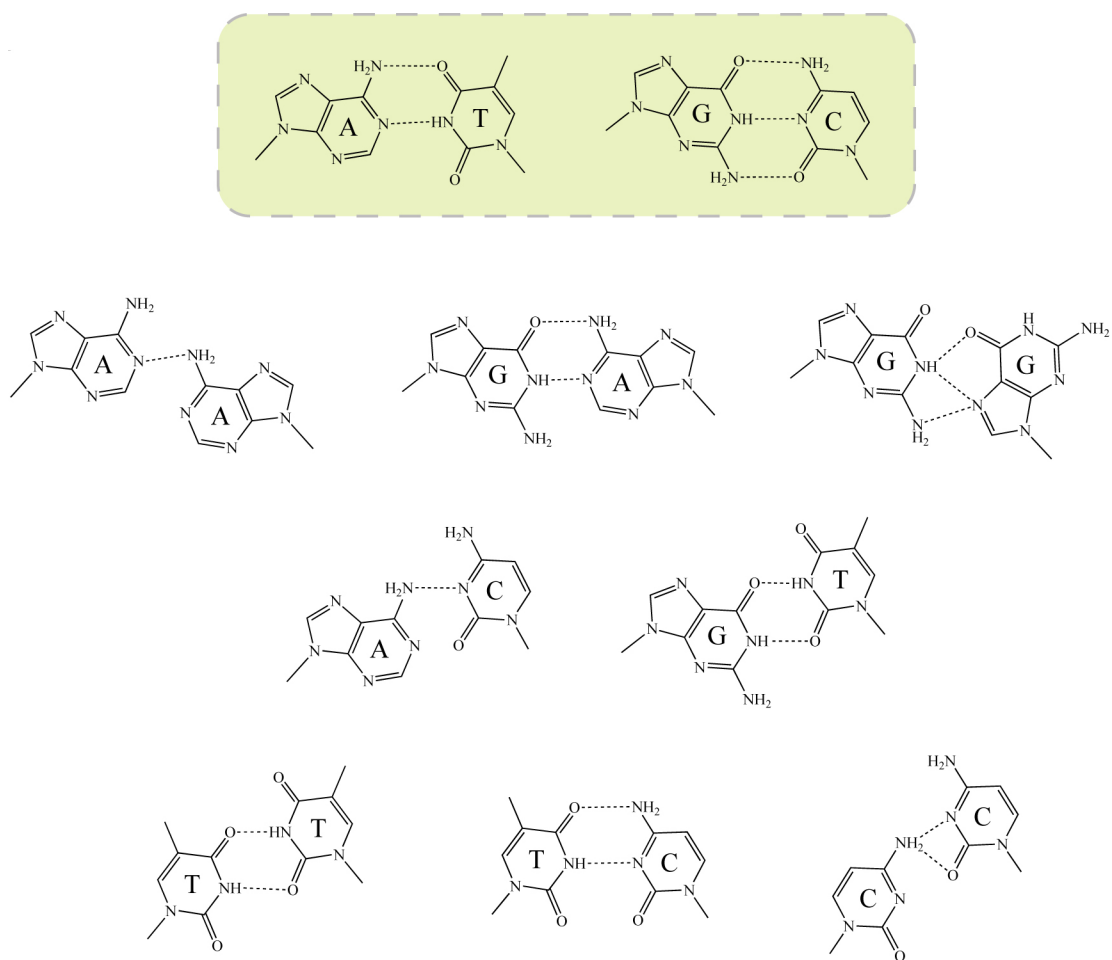


Figure 1.11: Mismatched DNA. The mismatched base pairs and their most probable hydrogen bonding interactions. The standard Watson-Crick base pairs are shown at the top, highlighted in green.

Several structures of DNA mismatches – specifically A•G, G•G, A•C, and G•T – in modified Drew-Dickerson dodecamers have been obtained by single crystal x-ray crystallography (**Figure 1.12**).^{87–91} In each, the DNA adopts a B-form structure without kinks or extrahelical bases. Some perturbation at the mismatch sites is observed, however; the mismatched bases themselves adopt unusual conformations in order to maximize hydrogen-bonding and π -stacking interactions.

Nuclear magnetic resonance studies have provided complementary insights into the structure of mismatched DNA; while NMR cannot offer the level of resolution and detail characteristic of crystal structures, the technique is performed under far more physiologically relevant conditions and, importantly, can provide information on base dynamics.⁹² Solution structures of various mismatched duplexes have confirmed an overall B-form structure. Further, experiments show that the hydrogen bonding schemes of certain mismatches (*e.g.* G•T) may change based on the identity of the base pairs flanking the mispair.^{93, 94} Most important, though, is the observation that mismatched bases are characterized by a higher rate of proton exchange than their matched counterparts. For this to be the case, mismatches must undergo a conformational change to expose the base-pairing face of each nucleotide to bulk solvent. Whether this behavior is a slight opening of the mispaired bases or the adoption of a fully extrahelical conformation is unknown. Regardless of the detailed mechanics, however, one thing is certain: this behavior is indicative of thermodynamic destabilization at mismatched sites.

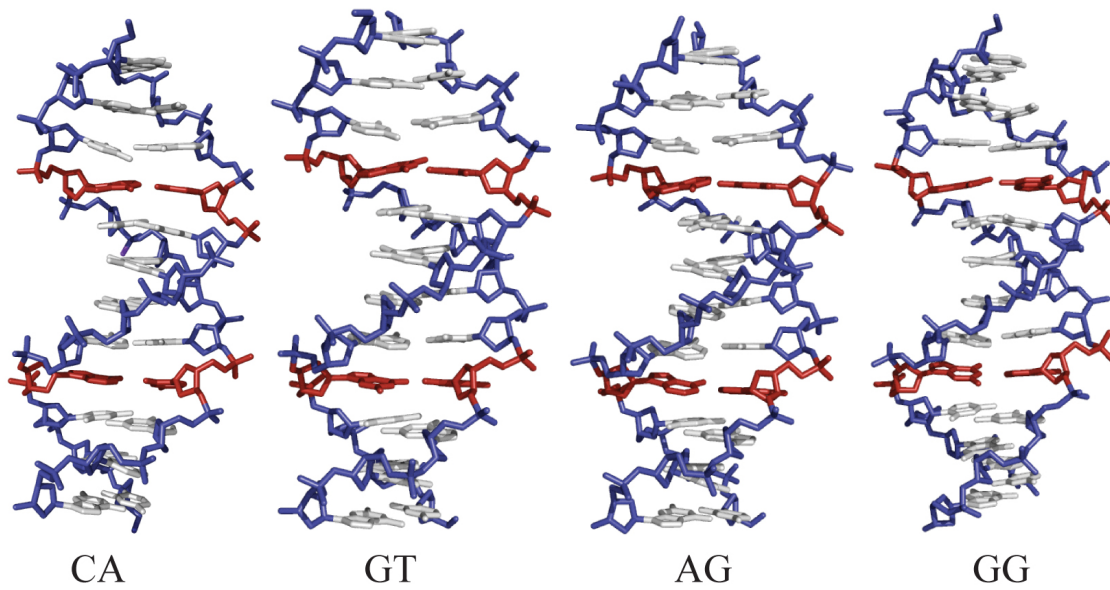


Figure 1.12: Crystal structures of mismatch-containing DNA duplexes. Each palindromic duplex is labeled with the mismatch it contains. While the mismatched bases appear slightly perturbed, the overall structure of the duplex is disrupted very little. The mismatches are shown in red.

1.7.1.2: THERMODYNAMICS

The energetics of single base mismatches have also been very thoroughly studied using both UV-Vis and NMR spectroscopy. UV-Vis measurements, which provide insight into the destabilizing influence a mismatch has on an oligonucleotide as a whole, have made the comparison of the stabilities of different mismatches quite easy. In general, then, a ranking of the stability of base pairs proceeds as follows: C•G > A•T > > G•G ~ G•T ~ A•G > > T•T ~ A•A > C•T ~ A•C > C•C.⁹⁴ The relative order does, admittedly, have some dependence on sequence context, but the trends generally remain similar.⁹⁵ The guanine-containing mismatches tend to be the most stable mispairs because of the particular ability of guanine to form hydrogen bonds, but they are still destabilized relative to Watson-Crick base pairs. The C•C mismatch is the most destabilizing mispair, a result of poor hydrogen-bonding and small aromatic surface area.

The combination of UV-Vis data with ¹H-NMR data has allowed for the creation of standard tables of ΔG° parameters for all base pairs in every sequence context (**Table 1.1**).⁹⁶⁻¹⁰⁰ The 5'-AXC-3' sequence provides an example (**Figure 1.13**). In this particular sequence context, C•G and A•T Watson-Crick base pairs stabilize the duplex by 3.52 and 2.44 kcal/mol, respectively. In contrast, a C•C mismatch destabilizes the duplex by 2.12 kcal/mol. Indeed, regardless of the numbers, in all cases replacing a matched base pair with a mismatch will destabilize the duplex

GX/CY	A	C	G	T
A	0.17	0.81	-0.25	-1.30
C	0.47	0.79	-2.24	0.62
G	-0.52	-1.84	-1.11	0.08
T	-1.44	0.98	-0.59	0.45

CX/GY	A	C	G	T
A	0.43	0.75	0.03	-1.50
C	0.79	0.70	-1.84	0.62
G	0.11	-2.17	-0.11	-0.50
T	-1.28	0.40	-0.2	-0.10

AX/TY	A	C	G	T
A	0.61	0.88	0.14	-1.00
C	0.77	1.33	-1.44	0.64
G	0.02	-1.28	-0.13	0.71
T	-0.88	0.73	0.07	0.69

TX/AY	A	C	G	T
A	0.69	0.92	0.42	-0.6
C	1.33	1.05	-1.30	0.97
G	0.74	-1.45	0.44	0.43
T	-1.00	0.75	0.34	0.68

Table 1.1: Thermodynamics of mismatches. ΔG° values (kcal/mol) for different internal mismatches with neighboring matched base pairs. In all cases, the Watson-Crick base pairs, highlighted in red, are more stable than any of the possible mismatches. To obtain a value for a mismatch, C•C for example, in a sequence context, say 5'-AXC-3', add 1.33 + 0.79 to obtain a total of 2.12 kcal/mol destabilization. X refers to the row, while Y refers to the column.

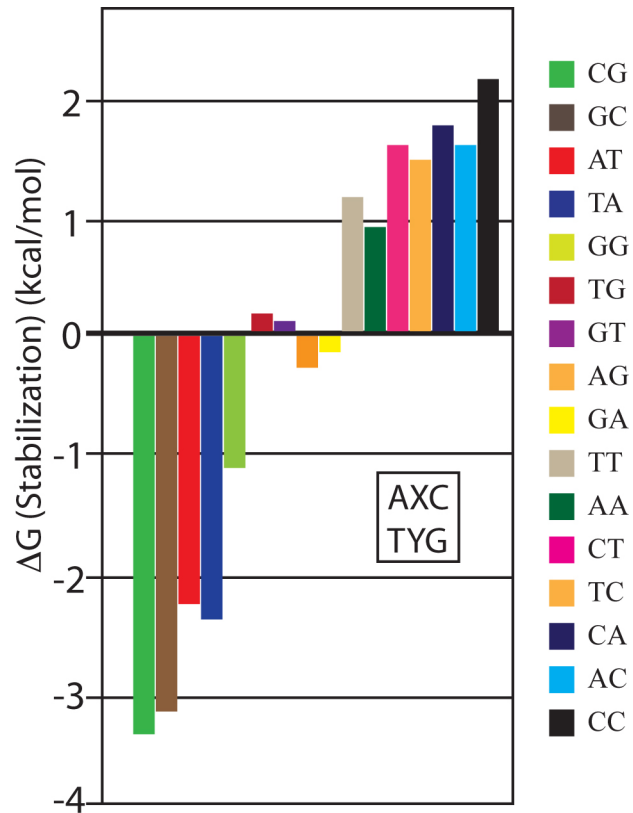


Figure 1.13: Thermodynamics of base pairs in a 5'-AXC-3' sequence context. The stabilization of different base pairs in the 5'-AXC-3' sequence is shown. The bars represent different base pairs (legend on the right), with negative ΔG° values net stabilizing and positive ΔG° values net destabilizing.

1.7.1.3: CAUSES

DNA replication is the most important source of mismatches *in vivo*.¹⁰¹ Alone, the catalytic domain of a DNA polymerase will misincorporate one in 10^4 bases.¹⁰² Needless to say, this is an unacceptably high level of infidelity for even the simplest organisms: upon a subsequent round of replication, unrepaired mismatches will become permanent mutations. To ensure the integrity of replication, most polymerases also employ proofreading domains which check the base pairs immediately after their incorporation and excise bases that have been incorrectly inserted. This dramatically increases the fidelity of the replication process to 1 incorrect base in $\sim 10^7$ – 10^8 bases.¹⁰³ The mismatch countermeasures do not stop here, however. Post-replication mismatch repair machinery (*vide infra*) can lower the misincorporation rate to as low as 1 base in 10^9 bases.

While the standard DNA replication process described above is quite accurate, under special circumstances, DNA synthesis can lead to higher rates of nucleotide misincorporation. The major polymerases involved in the replication of genomic DNA, Polymerase δ and Polymerase ϵ , are incapable of incorporating bases opposite chemically damaged bases.¹⁰⁴ When one of these two polymerases encounters such a site, they dissociate from the DNA and are temporarily replaced (100–1000 bases) by one of three translesion synthesis polymerases, Polymerase η , Polymerase ι , or Polymerase ξ .¹⁰⁵ These enzymes will readily incorporate a base opposite the chemically damaged site, but this functionality comes with a price; the translesion synthesis polymerases lack proof-reading domains and thus have far higher rates of nucleotide misincorporation than Pol δ and Pol ϵ .

A number of other, more minor processes can also create mismatches. During the genetic recombination of homologous chromatids, the sliding of the four-way Holliday junction intermediate can result in mismatch formation.¹⁰⁶ Cytosine deamination, a spontaneous chemical reaction in which the minor imine tautomeric form of cytosine is hydrolyzed to produce uracil, can create G•U mismatches.¹⁰⁷ These mismatches, if left unrepaired by the base excision repair machinery, will result in A•U mismatches and, ultimately, an A•T transversion. Interestingly, the action of an activated cytosine deaminase enzyme, AID, may be responsible for the creation of mismatches and consequent mutations during the process of intentional somatic hypermutation used by lymphocytes to increase genetic diversity in the production of immunoglobins.¹⁰⁷

1.7.1.4: REPAIR

Regardless of their source, mismatches are recognized and repaired *in vivo* by the endogenous mismatch repair (MMR) machinery.¹⁰⁸ In prokaryotes, the repair pathway is mediated by the MutS, MutL, and MutH proteins; in higher organisms, homologs of these enzymes play the central roles. The machinery detects a mismatch, excises a fragment of DNA containing the mismatch, and replaces approximately 1 kb of DNA.¹⁰⁹

In the prokaryotic pathway, the mechanistic details are murky, but a general sequence of events is accepted (**Figure 1.14**).¹¹⁰ First, a MutS dimer will recognize and bind a mismatched site in the DNA. The binding event attracts a MutL dimer. Next, in a poorly understood step, the MutS/L complex differentiates between parent and daughter strands

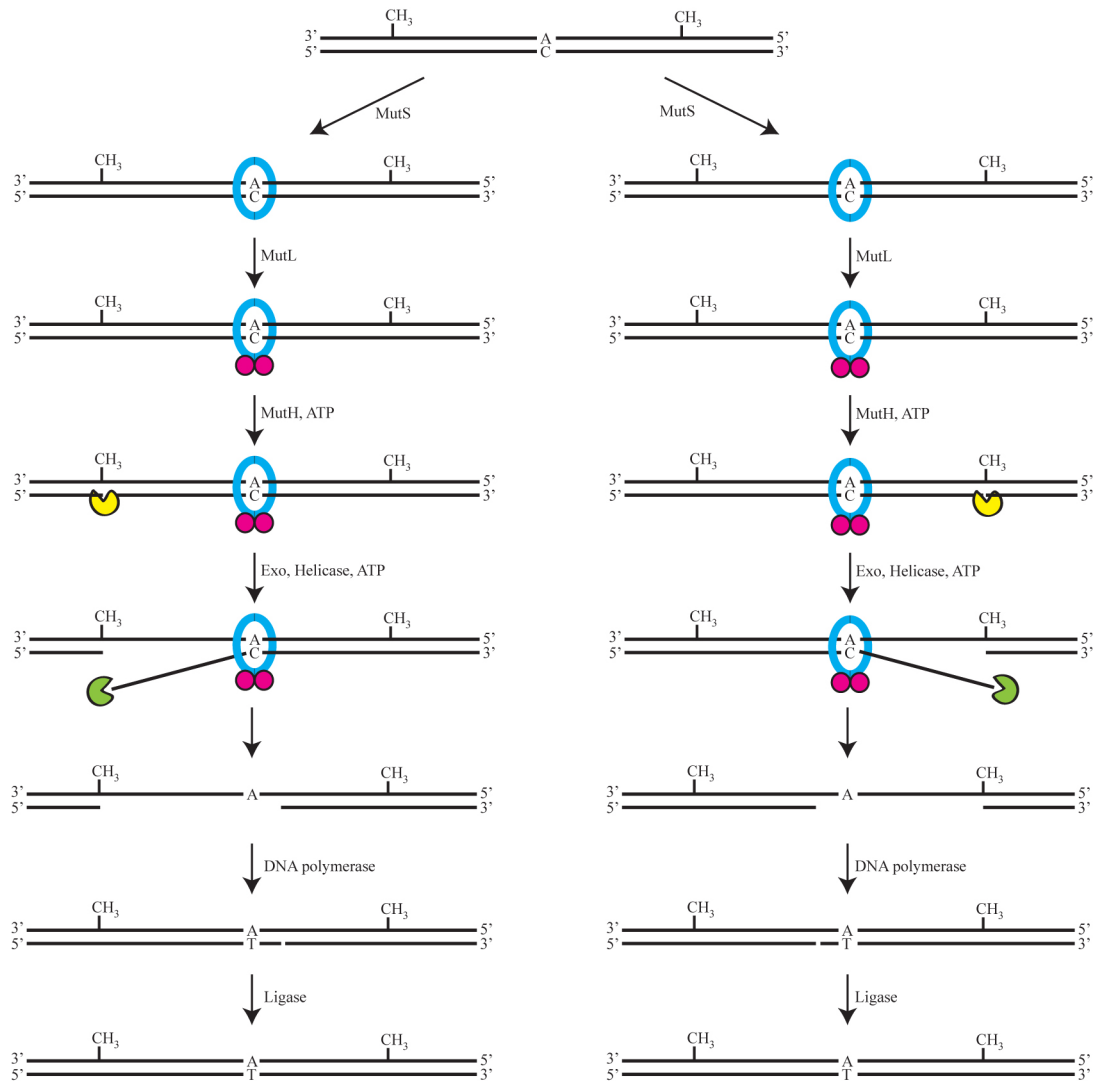


Figure 1.14: Mismatch repair in prokaryotes. A general scheme: (1) MutS recognizes and binds the mismatch; (2) MutL is recruited, and MutS/L identify the daughter strand; (3) MutH is recruited and nicks the daughter strand; (4) an exonuclease digests the nicked strand; (5) a DNA polymerase synthesizes a new daughter strand; (6) a ligase seals the nick, yielding intact, matched DNA.

and then recruits a third protein, the endonuclease MutH, to nick the daughter strand. The nicked strand is then digested by exonucleases traveling toward the mismatched site. Finally, a new DNA strand is synthesized by a polymerase, and the resultant nick is ligated to yield a fully repaired duplex. A similar, though slightly more complex, process governs mismatch repair in eukaryotes, with MSH2 replacing MutS, MLH1 replacing MutL, and an unknown endonuclease in place of MutH.¹¹¹

1.7.1.5: CONSEQUENCES

Upon replication, uncorrected mismatches will become permanent mutations. As we have discussed above, the cell has evolved a complex mismatch repair (MMR) machinery to counter this threat. Abnormalities in this machinery, however, lead to dire consequences: the genomic accumulation of mismatches and their consequent mutations create a high likelihood for cancerous transformations. Indeed, mutations in MMR genes have been identified in 80% of hereditary non-polyposis colon cancers; further, 15–20% of biopsied solid tumors have shown evidence of somatic mutations associated with MMR.¹¹² Moreover, MMR deficiency has been linked to resistance to common chemotherapeutic and antineoplastic agents.¹¹³ It thus becomes clear that the design, synthesis, and study of molecules able to specifically target single base mismatches is of tremendous importance to the development of new cancer diagnostics and therapeutics.

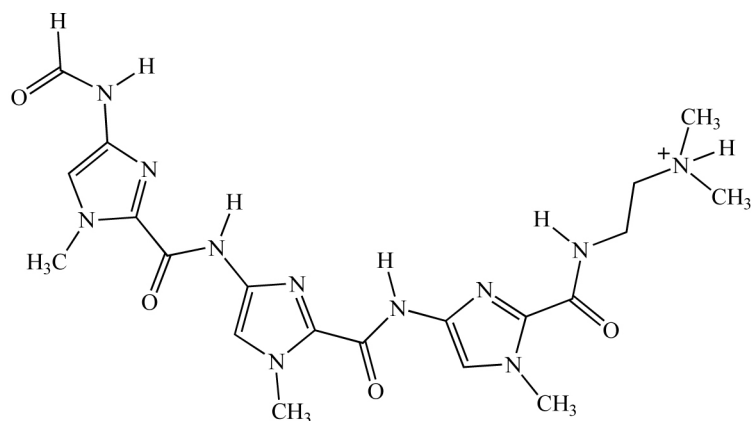
1.7.1.6: RECOGNITION BY SMALL MOLECULES

Given the biological importance of mismatches, it is not surprising that a number of organic, small molecule recognition agents have been developed. Two classes predominate: polyamides and naphthyridines.

Polyamides bind DNA through minor groove interactions, and the systematic modification of the chemical structural of polyamides has facilitated the recognition of almost any sequence.¹¹⁴ Mismatches are no exception. The polyamide f-ImImIm, for example, has been designed for the specific recognition of G•T mismatches (**Figure 1.15a**).^{115, 116} A dimer of the polyamide binds the mismatch through the minor groove with a relatively high affinity, approximately $5 \times 10^6 \text{ M}^{-1}$. However, the ultimate applicability of mismatch-binding polyamides is significantly limited by both their lack of generality and poor selectivity.

The second class of mismatch recognition agents, naphthyridines, has been studied extensively by the Nakatani and Saito groups. Originally, 2-amino-7-methylnaphthyridine was investigated for its ability to recognize and stabilize single guanine bulges in DNA.¹¹⁷ However, it was soon noted that dimers of naphthyridines are capable of recognizing a variety of different mismatches. For example, a naphthyridine dimer with an amide linker is capable of specific interactions with a G•G mismatch: the naphthyridines insert into the mismatch site, hydrogen bond with the mispaired guanines, and π -stack within the helix (**Figure 1.15b**). Somewhat surprisingly, a slightly different naphthyridine dimer with an alkyl linker is capable of the specific recognition of C•C, C•T, C•A, and T•T mismatches *via* a similar binding mode. In all cases, the binding

A.



B.

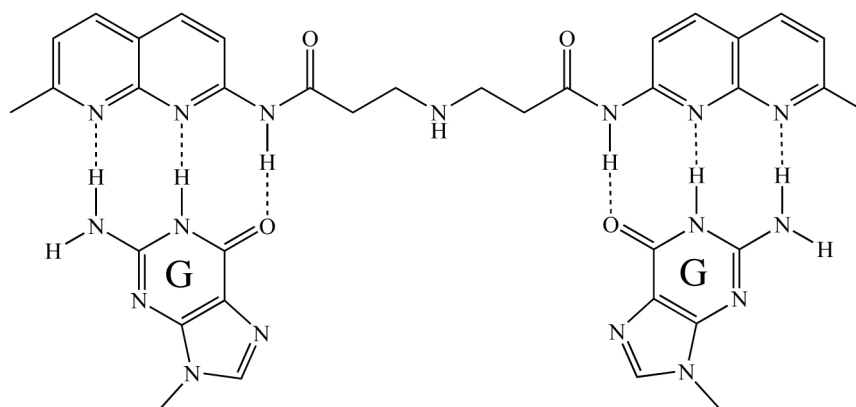


Figure 1.15: Organic mismatch recognition agents. (A) The polyamide f-ImImIm specifically recognizes G•T mismatches; (B) the amide-linked naphthyridine dimer specifically recognizes G•G mismatches.

constants hover around $1 \times 10^6 \text{ M}^{-1}$; however, these complexes, like polyamides, are limited by their lack of generality, modest selectivity, and photochemical inactivity.

1.7.2: RATIONAL DESIGN OF MISMATCH-SPECIFIC METAL COMPLEXES

Over the past ten years, much of our laboratory's work in molecular recognition has been focused on the design, synthesis, and study of metal complexes that selectively bind mismatched sites in DNA. When compared to sequence-specific metallointercalators, the design of mismatch-specific complexes presents a peculiar challenge. In this case, the recognition target is not a unique sequence but rather a type of site, specifically a region in the duplex that is thermodynamically destabilized by the mismatch's imperfect hydrogen-bonding. Indeed, an ideal mismatch recognition agent would bind all possible mismatched sites (C•C, C•A, A•G, etc.) without regard to the sequence context surrounding the mismatch. Taken together, these requirements dictate that the recognition elements of our mismatch-selective complexes must move from the ancillary ligands to the intercalating ligand.

Somewhat surprisingly, mismatch-specificity was achieved simply by replacing the non-specific phi ligand with the similar but more sterically expansive chrysene-5,6-quinone diimine (chrysi) ligand (**Figure 1.16**). Specifically, the chrysi ligand is 0.5 \AA wider than the span of matched DNA and 2.1 \AA wider than its parent phi ligand. Unlike the phi ligand, which is the ideal size for intercalation between the backbones of matched DNA, the chrysi ligand, with its additional fused ring, is too bulky to intercalate at stable, matched sites due to inevitable steric clash with the sugar rings of the DNA. Single base mismatches, it was proposed, would be a different story altogether, for at these

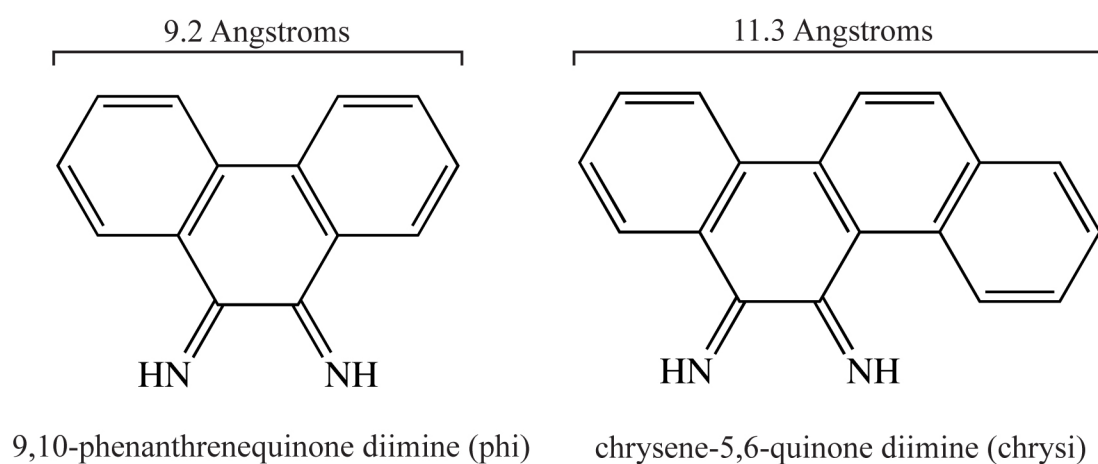


Figure 1.16: Structure of phi and chrysi ligands. The width of the phi ligand is well-suited for intercalation between the base pairs of well-matched DNA. The extra width of the chrysi ligand precludes binding at matched base pairs and instead confers selectivity for thermodynamically destabilized mismatched sites.

thermodynamically destabilized sites, the energetic benefit of the π -stacking ligand would outweigh the energetic cost of steric clash. In designing the complex, rhodium was again chosen as the metal primarily due its photophysical properties, most notably the ability of the non-specific rhodium complexes to promote strand scission upon irradiation.

1.7.3: RECOGNITION EXPERIMENTS

The first generation complex, $\text{Rh}(\text{bpy})_2(\text{chrysi})^{3+}$, was synthesized from $\text{Rh}(\text{bpy})_2(\text{NH}_3)_2^{3+}$ and chrysene-5,6-quinone via base-mediated condensation of the quinone onto the ammine ligands of the metal ion (**Figure 1.17a**).¹¹⁸ Initial photocleavage experiments showed that the complex does, indeed, bind mismatched sites and, upon photoactivation with UV-light, promotes direct strand cleavage of the DNA backbone adjacent to the mismatch site.¹¹⁹ The compound also proved to be remarkably selective; mismatches are bound at least 1000 times tighter than matched base pairs. A dramatic enantiomeric effect is also observed, with the Δ -enantiomer binding and cleaving extremely well and the Λ -enantiomer almost completely inactive. While the preference for the Δ -isomer binding to right-handed DNA was anticipated, the remarkably high enantioselectivity was unexpected, given the relatively small bipyridine ancillary ligands. Further experiments were performed to test the specificity of the complex. Photocleavage experiments employing alkaline agarose and denaturing polyacrylamide gels revealed that $\text{Rh}(\text{bpy})_2(\text{chrysi})^{3+}$ cleaves at, and only at, a single mismatch incorporated into a linearized 2725 base-pair plasmid.¹²⁰

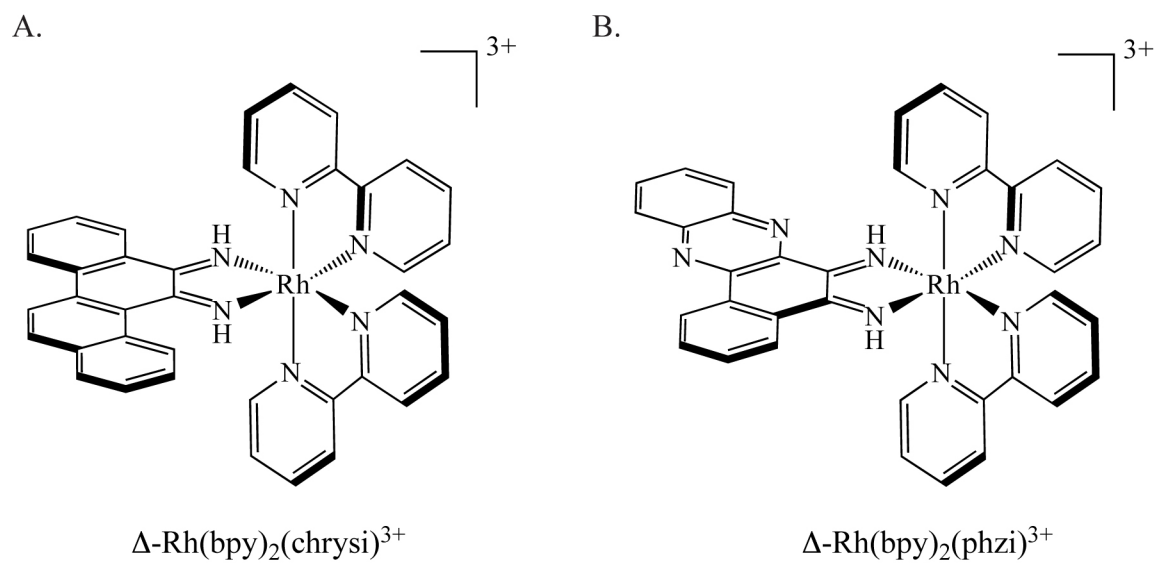


Figure 1.17: Structures of $\Delta\text{-Rh}(\text{bpy})_2(\text{chrysi})^{3+}$ and $\Delta\text{-Rh}(\text{bpy})_2(\text{phzi})^{3+}$

Subsequent investigations established that $\text{Rh}(\text{bpy})_2(\text{chrysi})^{3+}$ binds and cleaves 80% of mismatch sites in all possible sequence contexts.¹²¹ Furthermore, comparing the binding affinities of $\text{Rh}(\text{bpy})_2(\text{chrysi})^{3+}$ to independent measurements of mismatch destabilization revealed a clear correlation between mismatch stability and metal complex binding: in general, the more destabilized the mismatch, the tighter the binding. For example, the mismatch-selective binding constants of $\text{Rh}(\text{bpy})_2(\text{chrysi})^{3+}$ range from $3 \times 10^7 \text{ M}^{-1}$ for the dramatically destabilized C•C mismatch to $2.9 \times 10^5 \text{ M}^{-1}$ for the far more stable A•A mismatch.¹²⁰ Consistent with this relationship, $\text{Rh}(\text{bpy})_2(\text{chrysi})^{3+}$ almost completely fails to target the most stable mismatches, specifically those containing guanine nucleotides. In essence, the less destabilized mismatched sites “look” just like well-matched base-pairs to the metalloinsertor.

A second generation mismatch-specific metal complex, $\text{Rh}(\text{bpy})_2(\text{phzi})^{3+}$, was recently designed and synthesized (**Figure 1.17b**). The endocyclic nitrogens in the benzo[a]phenazine-5,6-quinone diimine (phzi) ligand enhance the π -stacking capability of the complex and thus raise its site-specific binding constant.¹²² For example, the binding constants of this complex for C•A and C•C mismatches were measured to be 0.3 and $1 \times 10^8 \text{ M}^{-1}$, respectively, affinities that allow for mismatch recognition and photocleavage at nanomolar concentrations. Importantly, the higher binding affinities are not accompanied by a concomitant decrease in selectivity, which remains at 1000-fold or greater. The increased affinity, however, is not sufficient to facilitate binding to the more stable G-containing mismatches.

1.7.4: STRUCTURE

While the above experiments provide comprehensive information on the range, strength, and specificity of mismatch recognition by $\text{Rh}(\text{bpy})_2(\text{chrysi})^{3+}$, they yield little, if any, information on the structure of the complex and DNA upon binding. Previous NMR and crystal structures of phi-bearing metallointercalators clearly indicate that these complexes bind by classical intercalation via the major groove.¹²³ There was, however, no guarantee that a mismatch recognition complex would bind DNA in a similar manner. Thus, the elucidation of the structure of $\text{Rh}(\text{bpy})_2(\text{chrysi})^{3+}$ bound to a mismatched site became of project of tremendous importance.

$\Delta\text{-Rh}(\text{bpy})_2(\text{chrysi})^{3+}$ was co-crystallized with a self-complementary oligonucleotide containing two A•C mismatches (5'-CGGAAATCCCG-3'). The structure was subsequently solved at atomic resolution (1.1 Å) using the single anomalous diffraction technique (**Figure 1.18**).⁵³ Quite surprisingly, the structure reveals *two* binding modes for $\text{Rh}(\text{bpy})_2(\text{chrysi})^{3+}$. In the crystal, not only is the complex bound to both mismatched sites as expected, but it is also intercalated at a matched site at the center of the oligonucleotide. However, a large volume of evidence, including a second crystal structure (*vide infra*), supports the idea that the binding observed at the matched site results entirely from crystal packing forces.

In stark contrast to other known metallointercalators, $\text{Rh}(\text{bpy})_2(\text{chrysi})^{3+}$ is bound to the mismatched DNA via the minor groove. Further, and perhaps more remarkably, the complex does not bind via classical *intercalation* but rather the previously unreported mode of *insertion*. Rather than stacking an intercalating ligand between base pairs,

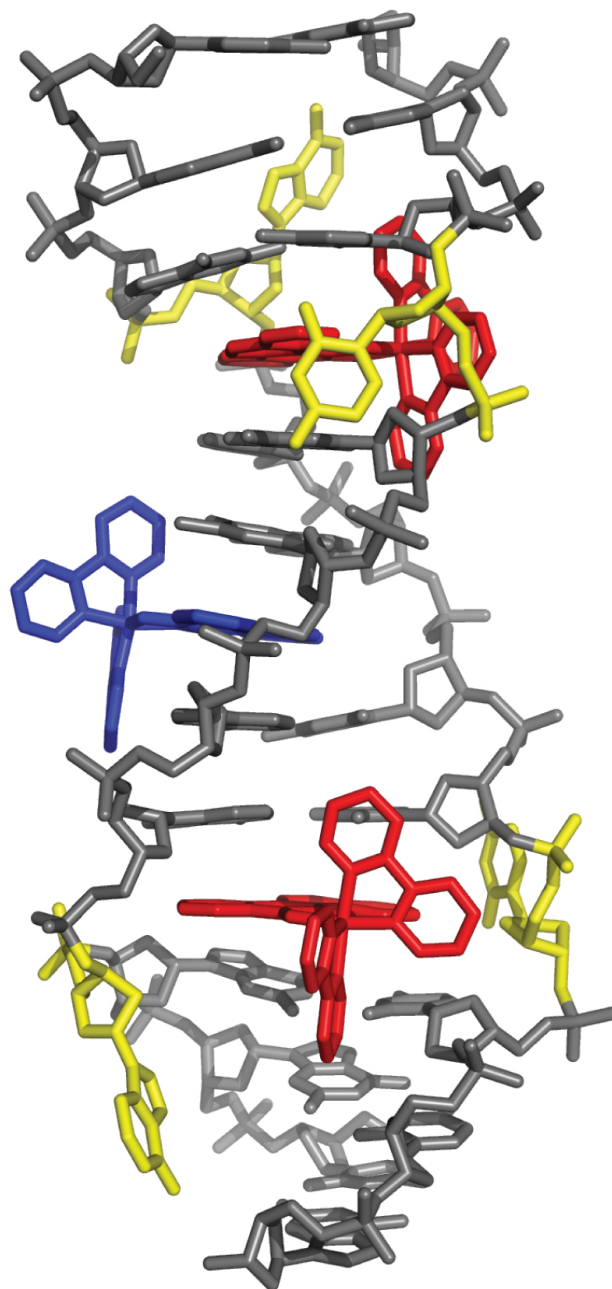


Figure 1.18: Crystal structure of Δ -Rh(bpy)₂(chrysi)³⁺ bound to a C•A mismatch. Crystal structure (1.1 Å) of the metalloinsertor (red) bound to a palindromic oligonucleotide containing two C•A mismatches (yellow). The centrally intercalated rhodium complex is shown in blue.

thereby prompting an increase in the rise of the DNA, $\text{Rh}(\text{bpy})_2(\text{chrysi})^{3+}$ completely ejects the mismatched nucleotides from the base-stack and replaces the ejected bases with its own sterically expansive ligand. Despite this insertion, the complex does not significantly distort the DNA; all sugars maintain a C2'-*endo* puckering, and all bases remain in the *anti*-configuration. Instead, the DNA accommodates the bulky ligand by opening its phosphate backbone slightly. The chrysi ligand is inserted quite deeply into the base stack, so much so that the rhodium is only 4.7 Å from the center of the helical axis, and the chrysi ligand is solvent accessible from the opposite major groove. Interestingly, the complex itself is perturbed very little, though some flattening of the chrysi ligand (perhaps to augment π -stacking) is observed. These structural observations have been independently verified in a recent NMR investigation.¹²⁴

The details provided by the crystal structure and NMR study help to explain three observations about which we could previously only hypothesize. First, the binding of the complex to the sterically smaller minor groove without an increase in rise explains the observed enantiospecific nature of recognition. Second, the minor groove insertion of the complex explains the different cleavage products created by $\text{Rh}(\text{bpy})_2(\text{chrysi})^{3+}$ and $\text{Rh}(\text{bpy})_2(\text{phi})^{3+}$ as observed via mass spectrometry.¹²⁵ The major groove binding mode of the metallointercalator positions it to cleave the DNA by abstracting the C2'H of the deoxyribose ring. Because it binds via the minor groove, $\text{Rh}(\text{bpy})_2(\text{chrysi})^{3+}$ is positioned to abstract preferentially the C1'H of the sugar adjacent to the mismatched site, and in this case, we see products consistent with C1'H abstraction. Finally, while we had previously demonstrated that the thermodynamic destabilization of the mismatch site is directly correlated to the binding affinity of the metal complex, the ejected bases

observed in the structure point to the concrete explanation. Since $\text{Rh}(\text{bpy})_2(\text{chrysi})^{3+}$ must displace the bases of the destabilized mismatched sites in order to bind the DNA, it follows that the more destabilized the site, the more easily the complex can eject the mispaired bases, and the tighter it can bind. Conversely, the complex cannot eject matched bases (or even more stable mismatched bases) because their hydrogen bonding interaction is too strong to allow for it.

1.7.5: DIAGNOSTIC APPLICATIONS

Considering the critical role of mismatches and mismatch repair deficiency in cancer susceptibility, the development of our unique recognition technology for diagnostic and therapeutic applications has also been a focus of our laboratory.

Fluorescence is a particularly attractive reporter in diagnostic applications and could be very useful in a sensitive early diagnostic for the detection of mismatches in genomic DNA. As a result, we have developed two different mismatch-specific fluorophores as potential diagnostics. The first probe, $\text{Ru}(\text{bpy})_2(\text{tactp})^{2+}$, sought to combine the DNA light-switch character of $\text{Ru}(\text{dppz})(\text{L})_2^{2+}$ complexes and the mismatch-specificity of the chrysi ligand in a single complex bearing a bulky chrysi/dppz hybrid ligand (**Figure 1.19a**).¹²⁶ However, while the complex does exhibit some light-switch behavior and mismatch-specific binding, the avid dimerization of the large aromatic ligand leads to non-specific fluorescence and thus dramatically limits its diagnostic potential. The second probe, a bifunctional conjugate combining a rhodium metalloinsertor with an organic fluorophore, will be discussed in the third chapter of this thesis.

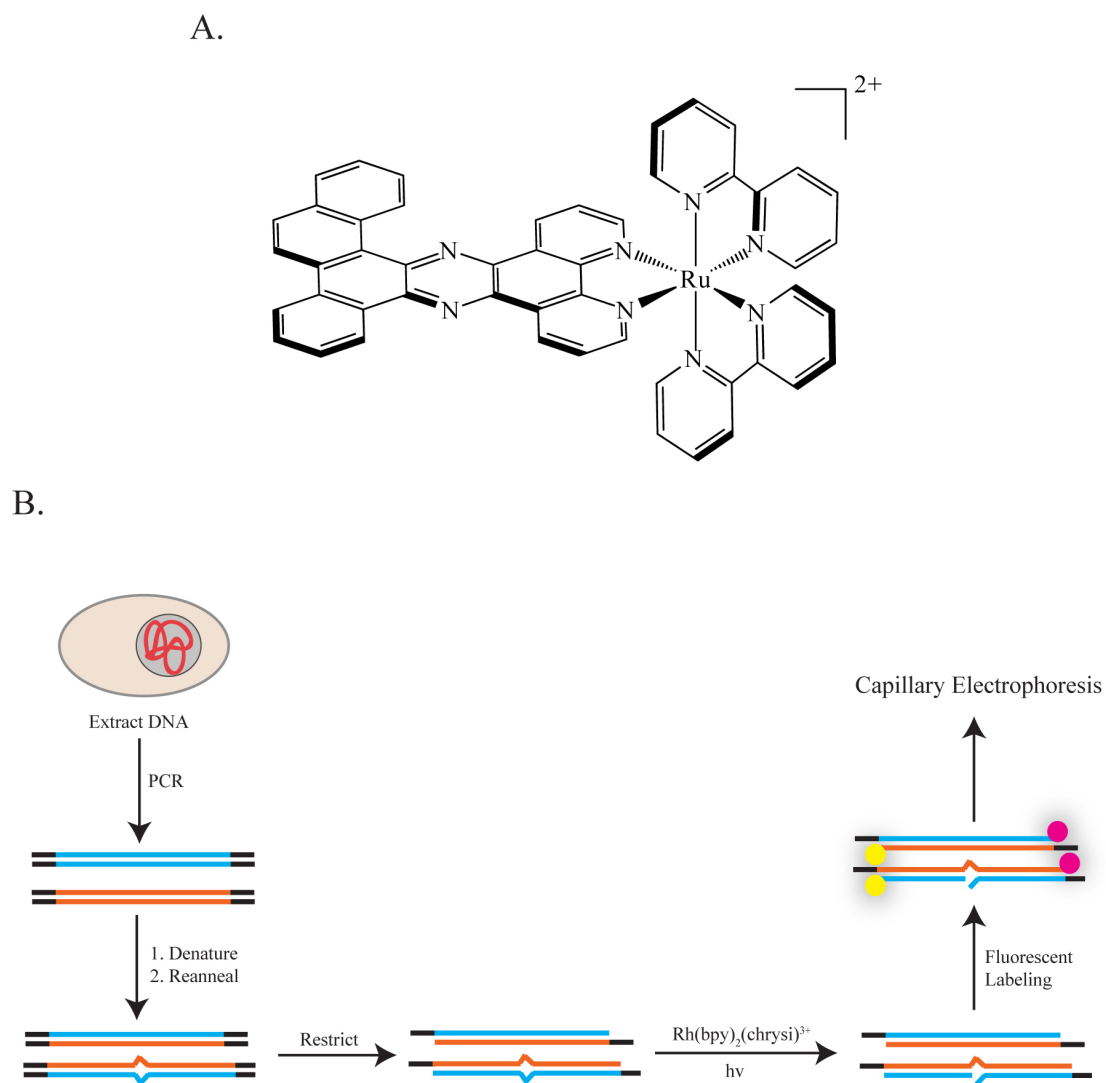


Figure 1.19: Diagnostic applications of metalloinsertors. (A) A complex designed as a mismatch-selective fluorophore, $\text{Ru}(\text{bpy})_2(\text{tactp})^{2+}$; (B) a schematic outline of a procedure for the detection of single nucleotide polymorphism using metalloinsertors

The site-specific photocleavage of both $\text{Rh}(\text{bpy})_2(\text{chrysi})^{3+}$ and $\text{Rh}(\text{bpy})_2(\text{phzi})^{3+}$ may also be exploited for diagnostic mismatch detection. Of course, the detection of mismatches in (labeled) oligonucleotides and synthetic plasmids does not hold particular diagnostic utility. Rather, the ideal system would allow for the quantification of the number of cleavage events (and thus mismatches) in the DNA from a particular cell sample or biopsy, thus indicating whether the tissue in question is MMR-deficient. $\text{Rh}(\text{bpy})_2(\text{phzi})^{2+}$, for example, has been used in conjunction with alkaline agarose electrophoresis to illustrate differences in site-specific cleavage frequencies in the DNA from MMR-proficient and -deficient cell lines. Further development of such a cleavage-based, whole-genome mismatch detection methodology using fluorescence is currently underway.

Mismatch-specific metalloinsertors have also been applied to the discovery of single nucleotide polymorphisms (SNPs).¹²⁷ SNPs are single base mutations that constitute the largest source of genetic variation in humans and can lead to variations in disposition to disease or response to pharmaceuticals. While other methodologies for SNP discovery exist, detection remains expensive, and false positive rates high.¹²⁸ In this application, a region of the genome suspected to contain an SNP is amplified via PCR, denatured, and then reannealed in the presence of a pooled sample (**Figure 1.19b**). If the region of interest had contained an SNP, the re-annealing process statistically generates a mismatch at the polymorphic site. The resultant mismatch-containing duplexes are then selectively cleaved via irradiation in the presence of $\text{Rh}(\text{bpy})_2(\text{chrysi})^{3+}$ or $\text{Rh}(\text{bpy})_2(\text{phzi})^{3+}$, fluorescently end-labeled, and analyzed via capillary gel electrophoresis. This new technique allows for the rapid identification of SNP sites with

single-base resolution. The methodology is further made useful by its sensitivity, for it allows for the detection of SNPs with allele frequencies as low as 5%.

1.7.6: THERAPEUTIC APPLICATIONS

The application of mismatch-specific metalloinsertors as a platform for new chemotherapeutics has also been of interest, especially considering that MMR-deficiency not only increases the likelihood of cancerous transformations but also decreases the efficacy of many common chemotherapeutic agents.¹¹³

Recently, it was discovered that both $\text{Rh}(\text{bpy})_2(\text{chrysi})^{3+}$ and $\text{Rh}(\text{bpy})_2(\text{phzi})^{3+}$ selectively inhibit cellular proliferation in MMR-deficient cells when compared to cells that are MMR-proficient.¹²⁹ Few small molecules have shown a similar cell-selective effect. Interestingly, enantiomeric differences are also observed associated with this inhibition. While the mismatch-binding, Δ -enantiomer of $\text{Rh}(\text{bpy})_2(\text{chrysi})^{3+}$ shows a high level of differential anti-proliferative effect, no such difference is seen using the non-binding Λ -enantiomer. This observation is important for two reasons. First, the mere presence of an enantiomeric difference strongly suggests that the causative agent is the intact complex, not some unknown degradation product or metabolite thereof. Second, the observation that the DNA-binding Δ - $\text{Rh}(\text{bpy})_2(\text{phzi})^{3+}$ and Δ - $\text{Rh}(\text{bpy})_2(\text{chrysi})^{3+}$ are the active enantiomers suggests that DNA mismatch binding plays at least some role in the anti-proliferative effect of these complexes. The surprise, however, was the observation that the biological effect occurs independent of irradiation with these complexes, even though they bind DNA only non-covalently.

More recently, the effect of ancillary ligand variation on the cytotoxicity of metalloinsertors has been explored.¹³⁰ A series of complexes with increasingly bulky ancillary ligands – $\text{Rh}(\text{NH}_3)_4(\text{chrysi})^{3+}$, $\text{Rh}(\text{bpy})_2(\text{chrysi})^{3+}$, $\text{Rh}(\text{HDPA})_2(\text{chrysi})^{3+}$, $\text{Rh}(\text{phen})_2(\text{chrysi})^{3+}$, and $\text{Rh}(\text{DIP})_2(\text{chrysi})^{3+}$ – was synthesized and assayed for their DNA binding capability. Perhaps not surprisingly, it was found that the smaller the ancillary ligands, the tighter the complex binds mismatched DNA; for example, while $\text{Rh}(\text{NH}_3)_4(\text{chrysi})^{3+}$ binds C•C mismatches with a binding affinity of greater than $1 \times 10^8 \text{ M}^{-1}$, $\text{Rh}(\text{DIP})_2(\text{chrysi})^{3+}$ binds the same mismatched site with an affinity of less than $1 \times 10^4 \text{ M}^{-1}$. The most interesting aspect of this study, however, comes to the fore when these complexes are employed in anti-proliferative assays: the tighter the complexes bind DNA (and thus the smaller the ancillary ligands), the greater the differential anti-proliferative effect in MMR-deficient and -proficient cells (**Figure 1.20**). This result not only further substantiates the role of mismatch binding in mediating the *in vivo* biological effect of these molecules but also marks a significant step forward in the development of more effective metalloinsertor-based chemotherapeutics. Currently, work is underway to understand the mechanism of cytotoxicity more fully and to maximize the differential effect of these complexes.

Several bifunctional, mismatch-specific conjugates have also been developed with a potential for chemotherapeutic application. In each, the rhodium moieties serve as the targeting vectors, delivering a cytotoxic cargo to mismatched DNA or, more generally, cells containing mismatched DNA, thereby tuning the reactivity of otherwise non-specific agents. Unlike $\text{Rh}(\text{bpy})_2(\text{chrysi})^{3+}$ or $\text{Rh}(\text{bpy})_2(\text{phzi})^{3+}$, these conjugates are

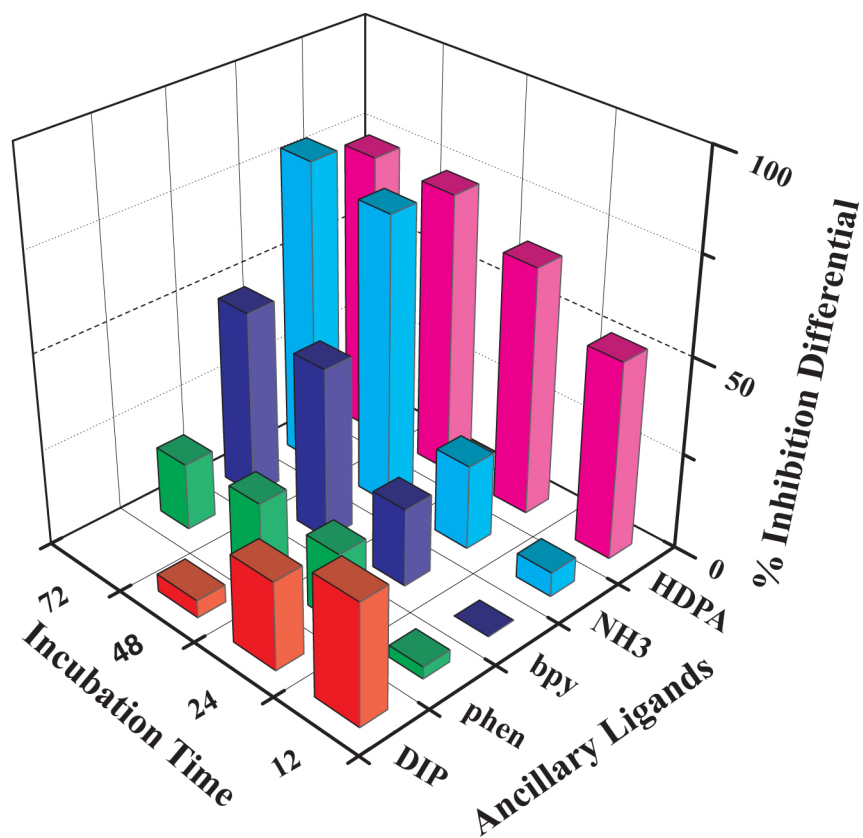


Figure 1.20: Differential anti-proliferative effects of metalloinsertors. A standard BrdU incorporation ELISA assay was employed to determine the anti-proliferative effects of a series of metalloinsertors as a function of ancillary ligand and incubation time.

trisheteroleptic, employing a tether-modified bipyridine ligand to establish the link between the two moieties. For example, in one conjugate the metalloinsertor is linked to a nitrogen mustard known to form covalent adducts at 5'-GXC-3' sites (**Figure 1.21a**).¹³¹ PAGE experiments with radiolabeled oligonucleotides confirm that the rhodium moiety successfully confers mismatch-selectivity on the alkylating agent. The two moieties neither abrogate nor attenuate each other's function. Significantly, independent of any chemotherapeutic application, this conjugate may also prove useful due to its ability to "mark" mismatch sites covalently.

Another bifunctional conjugate was created by linking a metalloinsertor moiety to an analogue of the well-known anticancer drug cisplatin, a Pt(II) complex that coordinates to single- and double-guanine sites in DNA and subsequently inhibits both transcription and replication (**Figure 1.21b**).¹³² Like its alkylator cousin, this conjugate succeeds in tuning the reactivity of the platinum subunit; upon binding a mismatched site, the platinum moiety then forms a covalent adduct with a nearby site. It is clear that it is the mismatch-selective Rh complex that dictates binding; the Pt moiety is seen to form interstrand as well as intrastrand crosslinks in the DNA, even though without linkage to the Rh center, cisplatin substantially prefers forming intrastrand crosslinks. Clearly, it is hoped that imparting mismatch-selectivity on such a potent anti-cancer drug may lead to a therapeutic agent against MMR-deficient cell lines.

Most recently, a third conjugate has sought to create a light-free, mismatch-specific DNA cleavage agent by tethering a $\text{Cu}(\text{phen})_2^+$ analogue to a selective metalloinsertor (**Figure 1.21c**).¹³³ The data reveal that this conjugate, like the others,

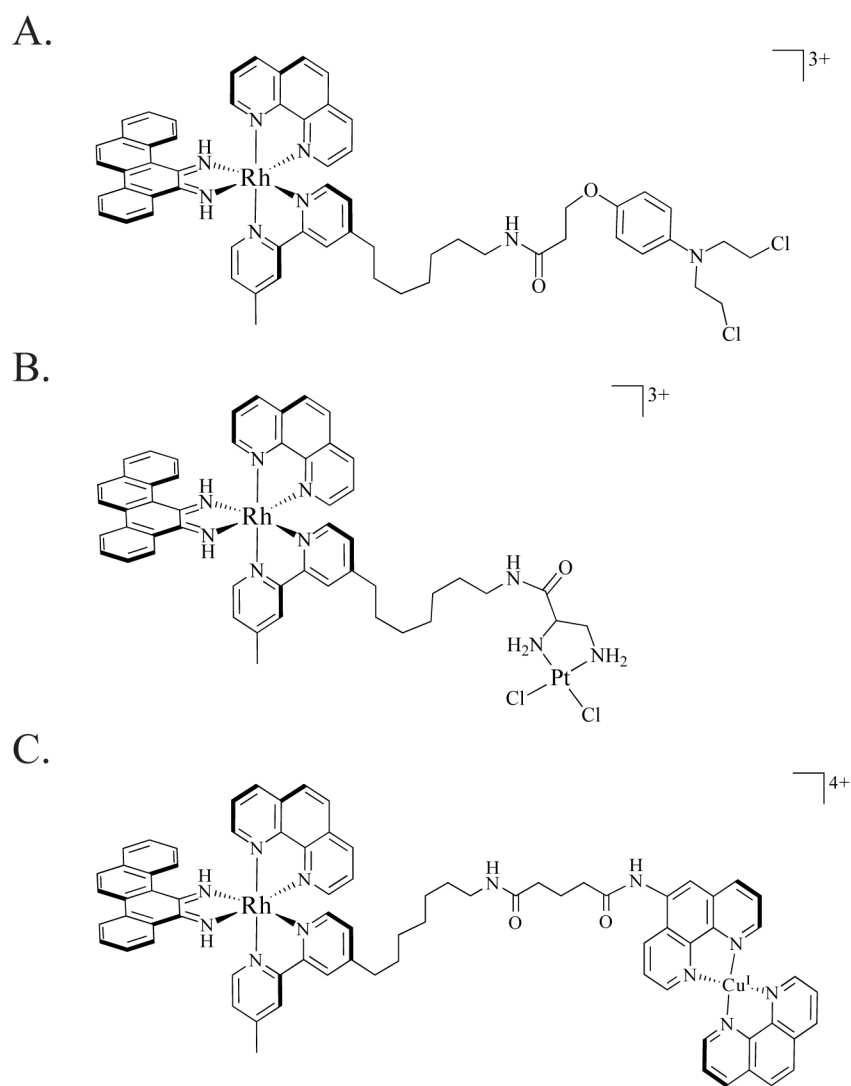


Figure 1.21: Three bifunctional, mismatch-selective conjugates. (A) A metalloinsertor-nitrogen mustard conjugate for mismatched strand-directed alkylation; (B) A metalloinsertor-cisplatin analogue conjugate for mismatched strand-directed platination; (C) A metalloinsertor- $\text{Cu}(\text{phen})_2^+$ conjugate for the light-free cleavage of mismatched DNA.

successfully directs the reactivity of the copper oxidant. Upon the addition of a stoichiometric reductant to convert Cu(II) to the active Cu(I), light-independent DNA backbone cleavage is observed near the mismatch site at concentrations for which no cleavage is seen with untethered $\text{Cu}(\text{phen})_2^+$ alone. Interestingly, however, the addition of the untethered rhodium metalloinsertor and copper moieties leads to similar, if not more pronounced, directed cleavage near the mismatched site, likely due to the slight opening of the minor groove caused by the Rh complex. Irrespective of potential chemotherapeutic applications, a mismatch-directed, DNA-cleaving conjugate could prove very useful, for it eliminates the need for a light source when cleaving mismatched sites. The antiproliferative effects of all three of these conjugates are currently being investigated, and the design and synthesis of other reactive conjugates are being explored (*vide infra*). Building upon the mismatch-selective binding of metalloinsertors through the design of bifunctional conjugates certainly offers new tools to probe MMR deficiencies in biological contexts.

1.7.7: CELLULAR UPTAKE

Whether for diagnostic or therapeutic applications, establishing the rapid and efficient cellular uptake of metal complexes is of fundamental importance. Cellular (and nuclear) delivery was first achieved through the conjugation of a D-octaarginine cell-penetrating peptide to the mismatch-binding rhodium complex (**Figure 1.22**).¹³⁴ The pendant peptide does not impair the ability of the rhodium moiety to bind and cleave mismatched sites; however, it does increase the non-specific binding by the complex, an

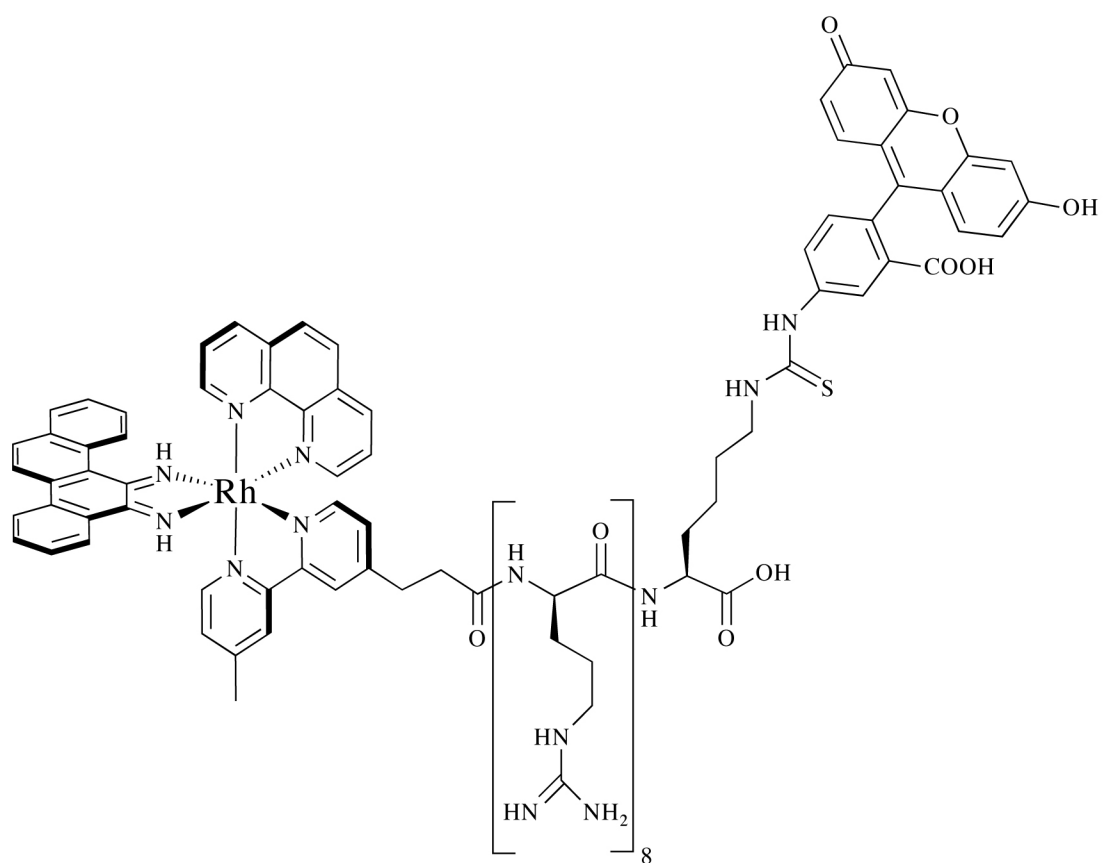


Figure 1.22. A trifunctional metalloinsertor-octaarginine-fluorophore conjugate

effect easily attributed to the strongly cationic character of the peptide. Confocal microscopy images of a similar trifunctional conjugate (this time containing a fluorophore in addition to rhodium and peptide) provide visual evidence for the rapid uptake of the conjugate into the nuclei of HeLa cells.

Despite the success of the peptide conjugate, it is becoming increasingly apparent that the cellular uptake properties of these metal complexes can be altered more simply by exploiting the modularity of their ancillary ligands. Indeed, systematic variation of the ancillary ligands offers a means to learn the characteristics of the metal complex that are essential to facilitate uptake. Using $\text{Ru(L)}_2(\text{dppz})^{2+}$ as a scaffold, it has been shown that increasing the lipophilicity of the ancillary ligands of the complex can dramatically enhance their uptake by HeLa cells. For example, data from both fluorescent cell sorting experiments and confocal microscopy confirm that $\text{Ru(phen)}_2(\text{dppz})^{2+}$ is more readily taken up than $\text{Ru(bpy)}_2(\text{dppz})^{2+}$, while the extremely lipophilic $\text{Ru(DIP)}_2(\text{dppz})^{2+}$ is taken up far better than the first two (**Figure 1.23**).¹³⁵ More recently, extensive mechanistic investigations have determined that passive diffusion is most likely the pathway for metal complex uptake.¹³⁶

Needless to say, the lessons learned here beg to be employed directly in the study of the differential anti-proliferative effects of $\text{Rh(bpy)}_2(\text{chrysi})^{3+}$ and $\text{Rh(bpy)}_2(\text{phzi})^{3+}$ in mismatch repair proficient and deficient cells; one might easily suppose that maximizing uptake will augment the differential biological effect. In this case, however, the situation becomes more complicated. That metalloinsertion occurs from the sterically constrictive minor groove dictates that the ligands of any *in vivo* therapeutic must be tuned to strike a

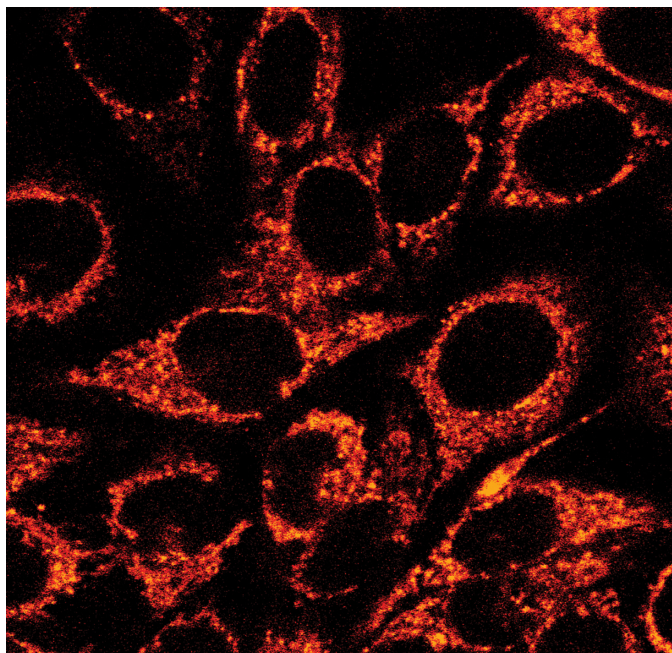


Figure 1.23. Confocal microscopy of HeLa cells incubated with Ru(DIP)₂(dppz)²⁺

delicate balance between affinity (favoring small ligands) and uptake (favoring larger ligands).

1.7.8: OUTLOOK

One clear conclusion to be drawn from the work described here is that the field has witnessed explosive growth and advancement over the years, from Lerman's initial suggestion of the non-covalent binding modes possible for small molecules and DNA to the design of bifunctional mismatch-specific conjugates. Yet surely, much remains to be done. From a design and synthesis standpoint, myriad possibilities exist, including the exploitation of different metals for their unique characteristics, the recognition of more complex and varied sites, and the expansion of the nascent metalloinsertor family. However, the intersection of this field with biology holds the greatest potential for growth. Despite some significant strides, the employment of these complexes in biological systems as probes, diagnostics, or therapeutics represents a largely untapped area with potentially tremendous value.

1.8: REFERENCES

1. Demeunynck, M.; Bailly, W. D. *Small Molecule DNA and RNA Binders: From Synthesis to Nucleic Acid Complexes*. Wiley–VCH: Weinheim, 2002.
2. Lippard, S. J.; Berg, J. M. *Principles of Bioinorganic Chemistry* University Science Books: Mill Valley, CA, 1994.
3. Erkkila, K. E.; Odom, D. T.; Barton, J. K. *Chemical Reviews* **1999**, *99* (9), 2777–2795.
4. Watson, J. D.; Crick, F. H. C. *Nature* **1953**, *171* (4356), 737–738.
5. Bloomfield, V. A.; Crothers, D. M.; Tinoco, I. *Nucleic Acids: Structure, Properties, and Functions*. University Science Books: Sausalito, California, 2000.
6. Izatt, R. M.; Christen, J. J.; Rytting, J. H. *Chemical Reviews* **1971**, *71* (5), 439–481.
7. Eichhorn, G. L.; Shin, Y. A. *Journal of the American Chemical Society* **1968**, *90* (26), 7323–7238.
8. Beer, M.; Moudrianakis, E. N. *Proceedings of the National Academy of Sciences of the United States of America* **1962**, *48* (3), 409–416.
9. Heitner, H. I.; Sunshine, H. R.; Lippard, S. J. *Journal of the American Chemical Society* **1972**, *94* (25), 8936–8937.
10. Dwyer, F. P.; Gyarfas, E. C.; Rogers, W. P.; Koch, J. H. *Nature* **1952**, *170* (4318), 190–191.
11. Jennette, K. W.; Lippard, S. J.; Vassilia, G. A.; Bauer, W. R. *Proceedings of the National Academy of Sciences of the United States of America* **1974**, *71* (10), 3839–3843.

12. Bond, P. J.; Langridge, R.; Jennette, K. W.; Lippard, S. J. *Proceedings of the National Academy of Sciences of the United States of America* **1975**, *72* (12), 4825–4829.
13. Howe–Grant, M.; Lippard, S. J. *Biochemistry* **1979**, *18* (26), 5762–5769.
14. Sigman, D. S. *Accounts of Chemical Research* **1986**, *19* (6), 180–186.
15. Meijler, M. M.; Zelenko, O.; Sigman, D. S. *Journal of the American Chemical Society* **1997**, *119* (5), 1135–1136.
16. Chen, C. H. B.; Milne, L.; Landgraf, R.; Perrin, D. M.; Sigman, D. S. *ChemBiochem* **2001**, *2* (10), 735–740.
17. Pope, L. E.; Sigman, D. S. *Proceedings of the National Academy of Sciences of the United States of America–Biological Sciences* **1984**, *81* (1), 3–7.
18. Sigman, D. S.; Bruice, T. W.; Mazumder, A.; Sutton, C. L. *Accounts of Chemical Research* **1993**, *26* (3), 98–104.
19. Chen, J. Y.; Stubbe, J. *Nature Reviews Cancer* **2005**, *5* (2), 102–112.
20. Stubbe, J.; Kozarich, J. W.; Wu, W.; Vanderwall, D. E. *Accounts of Chemical Research* **1996**, *29* (7), 322–330.
21. Boger, D. L.; Cai, H. *Angewandte Chemie–International Edition* **1999**, *38* (4), 448–476.
22. Burger, R. M. *Chemical Reviews* **1998**, *98* (3), 1153–1169.
23. Keck, M. V.; Manderville, R. A.; Hecht, S. M. *Journal of the American Chemical Society* **2001**, *123* (36), 8690–8700.
24. Dandrea, A. D.; Haseltine, W. A. *Proceedings of the National Academy of Sciences of the United States of America* **1978**, *75* (8), 3608–3612.

25. Barton, J. K.; Dannenberg, J. J.; Raphael, A. L. *Journal of the American Chemical Society* **1982**, *104* (18), 4967–4969.
26. Barton, J. K.; Danishefsky, A. T.; Goldberg, J. M. *Journal of the American Chemical Society* **1984**, *106* (7), 2172–2176.
27. Kumar, C. V.; Barton, J. K.; Turro, N. J. *Journal of the American Chemical Society* **1985**, *107* (19), 5518–5523.
28. Rehmann, J. P.; Barton, J. K. *Biochemistry* **1990**, *29* (7), 1701–1709.
29. Rehmann, J. P.; Barton, J. K. *Biochemistry* **1990**, *29* (7), 1710–1717.
30. Barton, J. K.; Raphael, A. L. *Proceedings of the National Academy of Sciences of the United States of America* **1985**, *82* (19), 6460–6464.
31. Barton, J. K. *Science* **1986**, *233*, 727–732.
32. Barton, J. K.; Basile, L. A.; Danishefsky, A. T.; Alexandrescu, A. *Proceedings of the National Academy of Sciences of the United States of America* **1984**, *82*, 6460–6468.
33. Barton, J. K.; Raphael, A. L. *Journal of the American Chemical Society* **1984**, *106* (8), 2466–2468.
34. Eriksson, M.; Leijon, M.; Hiort, C.; Norden, B.; Graslund, A. *Biochemistry* **1994**, *33* (17), 5031–5040.
35. Fu, P. K. L.; Bradley, P. M.; van Loyen, D.; Durr, H.; Bossmann, S. H.; Turro, C. *Inorganic Chemistry* **2002**, *41* (15), 3808–3810.
36. Schoentjes, B.; Lehn, J. M. *Helvetica Chimica Acta* **1995**, *78* (1), 1–12.
37. Hannon, M. J. *Chemical Society Reviews* **2007**, *36* (2), 280–295.
38. Oleksi, A.; Blanco, A. G.; Boer, R.; Uson, I.; Aymami, J.; Rodger, A.; Hannon, M. J.; Coll, M. *Angewandte Chemie–International Edition* **2006**, *45* (8), 1227–1231.

39. Uerpmann, C.; Malina, J.; Pascu, M.; Clarkson, G. J.; Moreno, V.; Rodger, A.; Grandas, A.; Hannon, M. J. *Chemistry—a European Journal* **2005**, *11* (6), 1750–1756.
40. Friedman, A. E.; Chambron, J. C.; Sauvage, J. P.; Turro, N. J.; Barton, J. K. *Journal of the American Chemical Society* **1990**, *112* (12), 4960–4962.
41. Friedman, A. E.; Kumar, C. V.; Turro, N. J.; Barton, J. K. *Nucleic Acids Research* **1991**, *19* (10), 2595–2602.
42. Jenkins, Y.; Friedman, A. E.; Turro, N. J.; Barton, J. K. *Biochemistry* **1992**, *31* (44), 10809–10816.
43. Hartshorn, R. M.; Barton, J. K. *Journal of the American Chemical Society* **1992**, *114* (15), 5919–5925.
44. Hiort, C.; Lincoln, P.; Norden, B. *Journal of the American Chemical Society* **1993**, *115* (9), 3448–3454.
45. Lincoln, P.; Broo, A.; Norden, B. *Journal of the American Chemical Society* **1996**, *118* (11), 2644–2653.
46. Tuite, E.; Lincoln, P.; Norden, B. *Journal of the American Chemical Society* **1997**, *119* (1), 239–240.
47. Franklin, S. J.; Barton, J. K. *Biochemistry* **1998**, *37* (46), 16093–16105.
48. Hudson, B. P.; Barton, J. K. *Journal of the American Chemical Society* **1998**, *120* (28), 6877–6888.
49. Dupureur, C. M.; Barton, J. K. *Journal of the American Chemical Society* **1994**, *116* (22), 10286–10287.

50. Collins, J. G.; Shields, T. P.; Barton, J. K. *Journal of the American Chemical Society* **1994**, *116* (22), 9840–9846.
51. Kielkopf, C. L.; Erkkila, K. E.; Hudson, B. P.; Barton, J. K.; Rees, D. C. *Nature Structural Biology* **2000**, *7* (2), 117–121.
52. Wang, A. H. J.; Nathans, J.; Vandermarel, G.; Vanboom, J. H.; Rich, A. *Nature* **1978**, *276* (5687), 471–474.
53. Pierre, V. C.; Kaiser, J. T.; Barton, J. K. *Proceedings of the National Academy of Sciences U. S. A.* **2007**, *103*, 429–434.
54. Greguric, I.; AldrichWright, J. R.; Collins, J. G. *Journal of the American Chemical Society* **1997**, *119* (15), 3621–3622.
55. Fry, J. V.; Collins, J. G. *Inorganic Chemistry* **1997**, *36* (13), 2919–&.
56. Collins, J. G.; Sleeman, A. D.; Aldrich–Wright, J. R.; Greguric, I.; Hambley, T. W. *Inorganic Chemistry* **1998**, *37* (13), 3133–3141.
57. Turro, C.; Bossmann, S. H.; Jenkins, Y.; Barton, J. K.; Turro, N. J. *Journal of the American Chemical Society* **1995**, *117* (35), 9026–9032.
58. Olson, E. J. C.; Hu, D.; Hormann, A.; Jonkman, A. M.; Arkin, M. R.; Stemp, E. D. A.; Barton, J. K.; Barbara, P. F. *Journal of the American Chemical Society* **1997**, *119* (47), 11458–11467.
59. Holmlin, R. E.; Stemp, E. D. A.; Barton, J. K. *Inorganic Chemistry* **1998**, *37* (1), 29–34.
60. Onfelt, B.; Lincoln, P.; Norden, B. *Journal of the American Chemical Society* **1999**, *121* (46), 10846–10847.

61. Onfelt, B.; Lincoln, P.; Norden, B. *Journal of the American Chemical Society* **2001**, *123* (16), 3630–3637.
62. Xiong, Y.; Ji, L. N. *Coordination Chemistry Reviews* **1999**, *185–6*, 711–733.
63. Sitlani, A.; Long, E. C.; Pyle, A. M.; Barton, J. K. *Journal of the American Chemical Society* **1992**, *114* (7), 2303–2312.
64. Fitzsimons, M. P.; Barton, J. K. *Journal of the American Chemical Society* **1997**, *119* (14), 3379–3380.
65. Copeland, K. D.; Lueras, A. M. K.; Stemp, E. D. A.; Barton, J. K. *Biochemistry* **2002**, *41* (42), 12785–12797.
66. Sitlani, A.; Barton, J. K. *Biochemistry* **1994**, *33* (40), 12100–12108.
67. Sitlani, A.; Dupureur, C. M.; Barton, J. K. *Journal of the American Chemical Society* **1993**, *115* (26), 12589–12590.
68. Pyle, A. M.; Long, E. C.; Barton, J. K. *Journal of the American Chemical Society* **1989**, *111* (12), 4520–4522.
69. Pyle, A. M.; Morii, T.; Barton, J. K. *Journal of the American Chemical Society* **1990**, *112* (25), 9432–9434.
70. Campisi, D.; Morii, T.; Barton, J. K. *Biochemistry* **1994**, *33* (14), 4130–4139.
71. Chow, C. S.; Barton, J. K. *Biochemistry* **1992**, *31* (24), 5423–5429.
72. Chow, C. S.; Behlen, L. S.; Uhlenbeck, O. C.; Barton, J. K. *Biochemistry* **1992**, *31* (4), 972–982.
73. Lim, A. C.; Barton, J. K. *Biochemistry* **1993**, *32* (41), 11029–11034.
74. Chow, C. S.; Hartmann, K. M.; Rawlings, S. L.; Huber, P. W.; Barton, J. K. *Biochemistry* **1992**, *31* (13), 3534–3542.

75. Krotz, A. H.; Kuo, L. Y.; Barton, J. K. *Inorganic Chemistry* **1993**, *32* (26), 5963–5974.
76. Krotz, A. H.; Kuo, L. Y.; Shields, T. P.; Barton, J. K. *Journal of the American Chemical Society* **1993**, *115* (10), 3877–3882.
77. Shields, T. P.; Barton, J. K. *Biochemistry* **1995**, *34* (46), 15037–15048.
78. Shields, T. P.; Barton, J. K. *Biochemistry* **1995**, *34* (46), 15049–15056.
79. Krotz, A. H.; Hudson, B. P.; Barton, J. K. *Journal of the American Chemical Society* **1993**, *115* (26), 12577–12578.
80. Terbrueggen, R. H.; Barton, J. K. *Biochemistry* **1995**, *34* (26), 8227–8234.
81. Terbrueggen, R. H.; Johann, T. W.; Barton, J. K. *Inorganic Chemistry* **1998**, *37* (26), 6874–6883.
82. Odom, D.; Parker, C. S.; Barton, J. K. *Journal of Inorganic Biochemistry* **1999**, *74* (1–4), 252–252.
83. Fu, P. K. L.; Bradley, P. M.; Turro, C. *Inorganic Chemistry* **2003**, *42* (3), 878–884.
84. Fu, P. K. L.; Turro, C. *Chemical Communications* **2001**, (03), 279–280.
85. Lerman, L. S. *Journal of Molecular Biology* **1961**, *3*, 18–30.
86. Marnett, L. J.; Plastaras, J. P. *Trends in Genetics* **2001**, *17*, 214–221.
87. Brown, T.; Hunter, W. N.; Kneale, G.; Kennard, O. *Proceedings of the National Academy of Sciences of the United States of America* **1996**, *83*, 2402–2406.
88. Hunter, W. N.; Brown, T.; Kennard, O. *Nucleic Acids Research* **1987**, *15*, 6589–6606.
89. Hunter, W. N.; Brown, T.; Kneale, G.; Anand, N. N.; Rabinovich, D.; Kennard, O. *Journal of Biological Chemistry* **1987**, *262*, 9962–9970.

90. Skelly, J. V.; Edwards, K. J.; Jenkins, T. C.; Neidle, S. *Proceedings of the National Academy of Sciences of the United States of America* **1993**, *90*, 804–808.
91. Drew, H. R.; Wing, R. M.; Takano, R.; Broa, C.; Tanaka, S.; Itakura, K.; Dickerson, R. E. *Proceedings of the National Academy of Sciences of the United States of America* **1981**, *78*, 2179–2183.
92. Arnold, F. H.; Wolk, S.; Cruz, P.; Tinoco, I. *Biochemistry* **1987**, *26*, 4068–4075.
93. Isaacs, R. J.; Rayens, W. S.; Spielmann, H. P. *Journal of Molecular Biology* **2002**, *319*, 191–207.
94. Peyret, N.; Seneviratne, P. A.; Allawi, H. T.; SantaLucia, J. *Biochemistry* **1999**, *38*, 3468–3477.
95. SantaLucia, J.; Hicks, D. *Annual Reviews in Biophysics and Biomolecular Structure* **2004**, *33*, 415–440.
96. Allawi, H. T.; SantaLucia, J. *Biochemistry* **1998**, *37* (26), 9435–9444.
97. Allawi, H. T.; SantaLucia, J. *Biochemistry* **1997**, *36* (34), 10581–10594.
98. Allawi, H. T.; SantaLucia, J. *Biochemistry* **1998**, *37* (8), 2170–2179.
99. Allawi, H. T.; Santalucia, J. *Nucleic Acids Research* **1998**, *26* (11), 2694–2701.
100. Allawi, H. T.; SantaLucia, J. *Nucleic Acids Research* **1998**, *26* (21), 4925–4934.
101. Kunkel, T. A. *Journal of Biological Chemistry* **2004**, *279*, 16895–16898.
102. Schaaper, R. M. *Journal of Biological Chemistry* **1993**, *268*, 23762–23765.
103. Drake, J. W.; Charlesworth, B.; Charlesworth, D.; Crow, J. F. *Genetics* **1998**, *148*, 1667–1686.
104. Kunkel, T. A. *Cancer Cell* **2003**, *3*, 105–110.
105. Lehmann, A. R. *FEBS Letters* **2005**, *579*, 873–876.

106. Gerton, J. L.; Hawley, R. S. *Nature Reviews Genetics* **2005**, *6*, 477–487.
107. Samaranyake, M.; Bujnicki, J. M.; Carpenter, N.; Bhagwat, A. S. *Chemical Reviews* **2006**, *106*, 700–719.
108. Iyer, R. R.; Pluciennik, A.; Burdett, V.; Modrich, P. *Chemical Reviews* **2006**, *106*, 302–323.
109. Kolodner, R. *Genes & Development* **1996**, *10* (12), 1433–1442.
110. Modrich, P. *Journal of Biological Chemistry* **2006**, *281* (41), 30305–30309.
111. Kolodner, R. D. *Trends in Biochemical Science* **1995**, *20*, 397–401.
112. Jacob, S.; Praz, F. *Biochimie* **2002**, *84*, 27–47.
113. Fink, D.; Aebi, S.; Howell, S. B. *Clinical Cancer Research* **1998**, *4* (1), 1–6.
114. Dervan, P. B.; Edelson, B. S. *Current opinion in Structural Biology* **2003**, *13*, 284–299.
115. Lacy, E. R.; Cox, K. K.; Wilson, W. D.; Lee, M. *Nucleic Acids Research* **2002**, *30*, 1834–1841.
116. Lacy, E. R.; Nguyen, B.; Le, M.; Cox, K. K.; Hartley, J. A.; Lee, M.; Wilson, W. D. *Nucleic Acids Research* **2004**, *32*, 2000–2007.
117. Nakatani, K.; Sando, S.; Saito, I. *Journal of the American Chemical Society* **2000**, *122*, 2172–2177.
118. Murner, H.; Jackson, B. A.; Barton, J. K. *Inorganic Chemistry* **1998**, *37* (12), 3007–3012.
119. Jackson, B. A.; Barton, J. K. *Journal of the American Chemical Society* **1997**, *119* (52), 12986–12987.

120. Jackson, B. A.; Alekseyev, V. Y.; Barton, J. K. *Biochemistry* **1999**, *38* (15), 4655–4662.
121. Jackson, B. A.; Barton, J. K. *Biochemistry* **2000**, *39* (20), 6176–6182.
122. Junicke, H.; Hart, J. R.; Kisko, J. L.; Glebov, O.; Kirsch, I. R.; Barton, J. K. *Proceedings of the National Academy of Sciences U. S. A.* **2003**, *100*, 3737–3742.
123. Hudson, B. P.; Dupureur, C. M.; Barton, J. K. *Journal of the American Chemical Society* **1995**, *117* (36), 9379–9380.
124. Cordier, C.; Pierre, V. C.; Barton, J. K. *Journal of the American Chemical Society* **2007**, *129*, 12287–12295.
125. Brunner, J.; Barton, J. K. *Journal of the American Chemical Society* **2006**, *128* (21), 6772–6773.
126. Ruba, E.; Hart, J. R.; Barton, J. K. *Inorganic Chemistry* **2004**, *43* (15), 4570–4578.
127. Hart, J. R.; Johnson, M. D.; Barton, J. K. *Proceedings of the National Academy of Sciences of the United States of America* **2004**, *101* (39), 14040–14044.
128. Rider, M. J.; Taylor, S. L.; Tobe, V. O.; Nickerson, D. A. *Nucleic Acids Research* **1998**, *26* (967–973).
129. Hart, J. R.; Glebov, O.; Ernst, R. J.; Kirsch, I. R.; Barton, J. K. *Proceedings of the National Academy of Sciences U. S. A.* **2006**, *103*, 15359–15363.
130. Ernst, R. J.; Song, H.; Barton, J. K. *Journal of the American Chemical Society* **2009**, *131* (6), 2359–2366.
131. Schatzschneider, U.; Barton, J. K. *Journal of the American Chemical Society* **2004**, *126* (28), 8630–8631.

132. Petitjean, A.; Barton, J. K. *Journal of the American Chemical Society* **2004**, *126* (45), 14728–14729.
133. Lim, M. H.; Lau, I. H.; Barton, J. K. *Inorganic Chemistry* **2007**, *46*, 9528–9530.
134. Brunner, J.; Barton, J. K. *Biochemistry* **2006**, *45* (40), 12295–12302.
135. Puckett, C. A.; Barton, J. K. *Journal of the American Chemical Society* **2007**, *129* (1), 46–47.
136. Puckett, C. A.; Barton, J. K. *Biochemistry* **2008**, *47* (45), 11711–11716.